Abstract

Centrifugal casting process is most widely used for production of pipes, cylinder liners, brake drums, flywheels and other axis-symmetric parts, in which molten metal is poured at suitable temperature into rapidly rotating mold. The defects in centrifugal castings are mainly related to the solidification process. However, it is very difficult to determine the temperature distribution and solidification time by experimental techniques in centrifugal casting. Their estimation is a complex problem mainly because the moving particles disturb temperature equilibrium.

This project focuses on mathematical modeling of centrifugal casting process to estimate solidification time and the influence of other process parameters on the solidification time and temperature distribution. Since the solidification process is related to the heat transfer of the casting-mold-ambient system, numerical simulation is an effective method. The mathematical model for the solidification of centrifugal castings has been formulated by both Fixed Domain Method and Variable Domain Method. Numerical simulation of modeled equations using Finite Difference Technique has been attempted in the present study. The developed model is implemented in computer program and results have been obtained for both temperature distribution in casting and mold regions, and total solidification time of castings. These results are compared with literature, as well as results obtained by Ansys. The major advantage of Variable Domain method is that the position of solid-liquid interface can be found at any instant of the time.

Contents

List of Figures

List of Tables

Nomenclature

m	Mass of metal being poured (kg)
ω	Rotational speed of mold (rpm)
H	Heat content (J/kg)
ΔH	Heat of fusion (J/kg)
T_d	Standard temperature (0 ^{0}C)
k	Thermal conductivity (cal/cm sec ^{0}C)
k_I	Thermal conductivity of ingot (W/m ^{0}C)
k_M	Thermal conductivity of mold (W/m ^{0}C)
k_d(I)	Thermal conductivity of ingot at 0 ^{0}C
k_d(M)	Thermal conductivity of mold at 0 ^{0}C
K	Thermal conductivity of insulating material (W/m ^{0}C)
C	Specific heat (J/ kg ^{0}C)
C_I	Specific heat of ingot (J/ kg ^{0}C)
C_M	Specific heat of mold (J/ kg ^{0}C)
ρ	Density (kg/m^3)
ρ_I	Density of ingot (kg/m^3)
ρ_M	Density of mold (kg/m^3)
d	Thickness of coating layer (m)
d1	Thickness of casting (m)
d2	Thickness of mold (m)
β	Damping coefficient of heat flux within coating layer due to air gap formation
ε	Emissitivity
ε_I	Emmisivity of ingot
ε_M	Emissivity of mold
σ	Stefan – Boltzmann's constant (W/m^2 k^4)
h_2	Heat transfer coefficient at the outer surface of mold (W/m^2 ^{0}C)
h1	Heat transfer coefficient at inner surface of casting (W/m^2 ^{0} C)
r	Radius (m)
R_{ic}	Inner radius of Ingot (m)
R_{oc}	Outer radius of ingot (m)

R_{im}	Inner radius of mold (m)
R_{om}	Outer radius of mold (m)
Δr_1	Size increments in the radial direction of ingot (m)
Δr_2	Size increments in the mold (m)
t	Time (sec)
Δt	Time increment (sec)
w	Heat flux during time increment Δt (J/m^2)
s(t)	Solidified thickness of ingot (m)
T	Temperature (^0C)
T_f	Solidification front temperature (^0C)
T_m	Temperature of steel mold (^0C)
T_L	Liquidus temperature of base alloy (^0C)
T_S	Solidus temperature of base alloy (^0C)
T_p	Pouring Temperature (^0C)
T_{lc}	Temperature of liquid region of casting (^0C)
T_{sc}	Temperature of solid region of casting (^0C)
T_a	Ambient temperature (^0C)
α	Thermal diffusivity (m^2sec^{-1})
Re	Reynold Number
Nu	Nusselt Number
Pr	Prandlt Number
C_D	Coefficient of drag
H_{ps}	Psuedo-Enthalpy (J/kg)
I	Solid-liquid interface
R_F	Radiation factor
v_I	Interface velocity (m/sec)
ϕ	Function expressed in terms of $\phi = \int_{Td}^{T} \frac{k}{k_d} dT$
θ	Dimensionless Temperature
Ste	Stefan Number $Cp\ (T_s-T_a)/\Delta H$
F_b	Body forces term in momentum equation (N)
f_l	Liquid fraction
P	Pressure (N/m^2)

Chapter-1

Introduction

1.1 General Introduction

Metal casting is the oldest industries in the human society. The art of foundry is as ancient as the dawn of the civilization. Even the craftsmen of the Greek and Roman civilization had practiced the art of foundry. A casting may be defined as a "metal object obtained by allowing molten metal to solidify in a mold", the shape of the object being determined by the shape of the mold cavity [Hiene, 1955]. The strength of the foundry industry lies in the fact that, the casting process allows metals to take the shapes that will serve the need of the humans.

Casting, or reforming materials by heating, melting and molding, can be traced back in history six thousand years. As civilization progressed and the use of metals became more advanced, the technology of casting metals advanced as well. As foundry industries began to demand higher yields and better physical properties from cast metal products, casting processes became more specialized.

The centrifugal casting method was developed after the turn of the 20^{th} century to meet the need for higher standards. The process of centrifugal casting differs from static casting in that the mold itself is spinning during the time, casting is solidifying. Centrifugal castings are usually poured while the mold is spinning; however, for certain applications, particularly in the case of a vertical casting, it is sometimes preferable that the mold be stationary when pouring begins. The machine then accelerates the speed of the rotating mold either during the filling of the mold or after completion of pouring. In other cases, such as horizontal centrifugal casting, it is often desirable to have the mold rotating at a lower speed during pouring, followed by rapid acceleration to a higher speed during the solidification period. The application of centrifugal force to a molten metal as it solidifies can be used to achieve a dense, sound casting. The centrifugal casting process is most widely used for manufacturing of cast iron tubes, pipes, cylinder liners and other axis-symmetry parts.

1.1.1 Centrifugal Casting

The centrifugal casting process consists of pouring the molten metal at a suitable temperature into a rapidly rotating mould or die. It is essential that pouring temperature of molten metal should be high enough to enable it to reach the farthest point in the mould before solidification commence. The axis of rotation of mould may be horizontal, vertical or slightly inclined. The centrifugal force imparted to molten metal enables it to be picked up and held in contact with the rotating mould. The mould is allowed to rotate till the casting is completely solidified. Thus the outer shape of casting takes the shape of the inside of the mould and the bore of casting is truly circular and concentric with axis of rotation. The thickness of casting is determined by the quantity of molten metal poured, and the length by the length of mold between two end plates. In case of centrifugal casting, there is no need of runners and risers [Paranjpe, 2001]. The metal in the bore serves as riser. Therefore, the yield from centrifugal casting is much higher than normally obtained in gravity poured castings because there are neither separate gates nor risers. The castings thus produced also have a high density than that of gravity poured castings, and have the superior mechanical properties [Paranjpe, 2001].

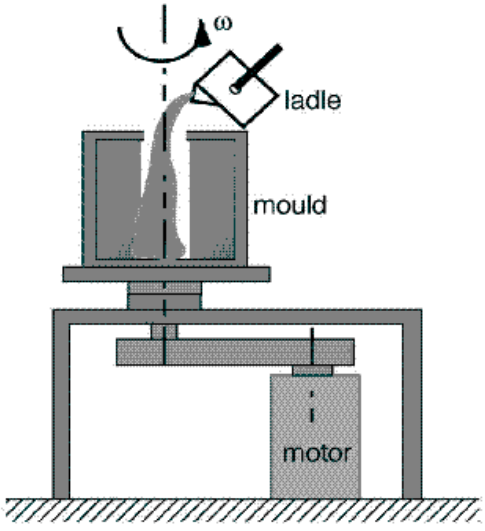

Fig1.1. Schematic of centrifugal casting process [Gao et al, 2000]

1.1.2 Methods of Centrifugal Casting [Janco, 1988]

There are three methods for the utilization of centrifugal force for casting. All are loosely referred to as “centrifugal casting”.

1.1.2a True Centrifugal Casting

No core is used in this method; essentially all of the heat is extracted from the molten metal through the outer mold wall. The poor thermal conductivity of the air in contact with the internal diameter results in little heat loss from this direction. Thus, perfect directional solidification is obtained from outer surface to inner one and grain growth is typically columnar. Because of favorable thermal gradients, in addition to the outward centrifugal force acting upon the molten metal, each successive increment of metal to solidify is fed by the residual liquid metal in contact with it, until solidification is complete. Under proper conditions, shrinkage porosity is non-existent.

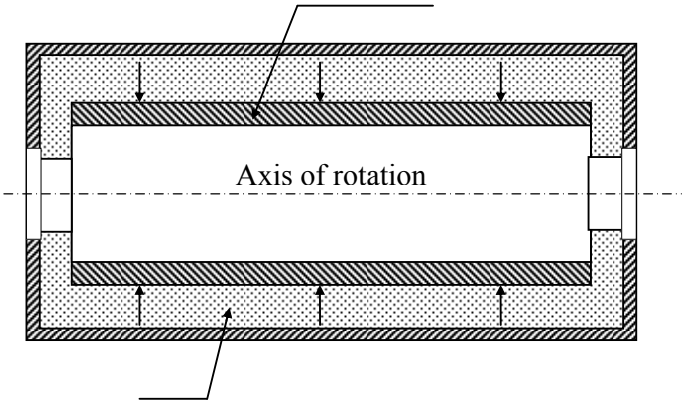

Fig 1.2. True Centrifugal Casting [Janco, 1988]

1.1.2b Semi-Centrifugal Casting

This is very similar to true centrifugal casting, except core is used in this method, due to the irregular contour of the internal bore. Solidification occurs in both inward and outward directions, with the consequent problem of centerline soundness. By the application of centrifugal force feeding is enhanced, and is equivalent to the use of very high risers. Gates of various types may be used, some of which serve as riser and

others for direction of molten metal into the mold cavity. This method is adaptable to a wide variety of cast parts such as jaw clutches, sheaves, gear blanks, casing heads, and flanges. It is also used for the production of castings, which have very thin metal sections.

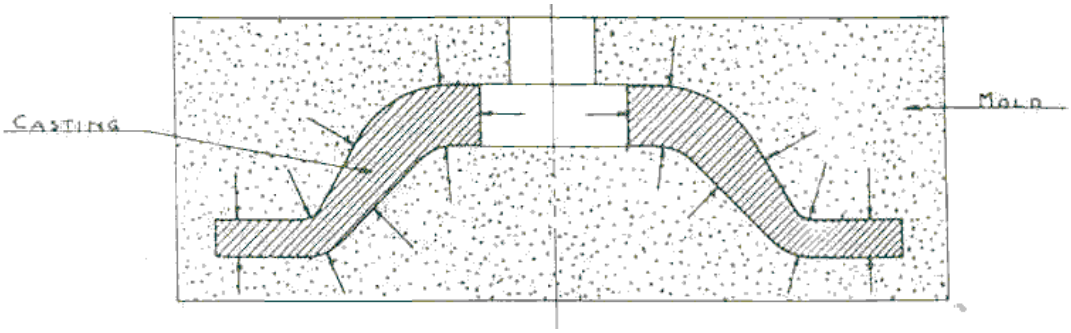

Fig1.3. Semi-Centrifugal Casting Method [Janco, 1988]

1.1.2c Centrifuge or Pressure Casting

In this method (usually done vertically but sometimes horizontally), there is a central sprue at the axis of rotation of the mold. Mold cavities are clustered about the central sprue in a symmetrical array, each connected to sprue by one or more radial gates. It is clear that since conditions are not designed to promote ideal directional solidification, it is necessary to apply skills in gating to promote solidification from remote points of casting toward the gate. Usually, only small castings such as unions, valve bodies, gates, plugs, and intricate parts are cast by this method.

Fig1.4. Five casting centrifuged in one mold [Janco, 1988]

1.1.3 Applications of Centrifugal Casting

Centrifugal castings are used over a broad field of application and the process allows the manufacture of components in many alloy types, both ferrous and non-ferrous [Cumberland, 1963],

- Rings, flanges and compressor casings are cast in martensitic and austenitic heat-resisting steels and nickel-rich alloys for the aircraft industry.
- Steam-turbine bearing-shells in leaded nickel bronze.
- Reducing roller for steel-rolling mills in alloy iron, spheroidal-graphite iron and carbon-steel.
- Corrosion-resisting rolls for the textile and cellophane industries in stainless steel.
- Cylinder liners, gear blanks and piston-ring blanks in all grade of grey iron for the motor-car industry.
- Rollers, ball or plain bearings in phosphor-bronze and other copper-rich alloys for the engineering industries.
- Switch-gear components in high-conductivity copper for the electrical engineering industries.

1.1.4 Working principle of process

In case of horizontal casting machine, the molten metal is poured in a mold, spinning around a horizontal axis at a sufficiently high speed of rotation. As soon as the poured molten metal comes in contact with the rapidly rotating mold, it is picked up and moves along with the rotating die and subjected to a centrifugal force, which is several times of gravitational force. This centrifugal force is enough to make it stay in contact with the mold against gravity, even when it is at top-most position. The minimum speed of rotation to make the molten metal in contact with the mold is that, which results in a centrifugal force of at least fifty times the force of gravity. As more metal is poured, it follows the same pattern and more such layers are held in contact with the inner surface of the mold against the gravity, till all the metal has been poured. The mold is allowed to rotate continuously at the high speed till the poured metal has completely solidified.

On vertical centrifugal casting machines to avoid the taper on the inside diameter of casting such speed of rotation is adopted that results in centrifugal force of 75G, based on the inside diameter of casting being made.

1.1.5 Advantages

Centrifugal casting provides various advantages over static casting, which are listed below [Jones, 1970, Choi et al, 1989]:

1. Effect of solidification shrinkage is progressively transferred to the inner bore.
2. Lower pouring temperatures are possible than those used for static castings.
3. High casting yield, since conventional running and gating systems are eliminated, can reach 96 percent and over in some application.
4. Compared with static castings, thermal gradient is much steeper due to unidirectional heat flow, this result in the characteristic columnar grains, compared with the equiaxed structure of sand casting.
5. The steep thermal gradient, especially with metal moulds gives rapid solidification and therefore fine grain-size.
6. Clean metal: When spun, the impurities such as dirt, sand slag, and gas pockets, since they are lighter, will collects on the inner surface of the central hole, where it can easily be removed by machining.
7. Dense metal: Since the molten metal solidifies under pressure, a dense metal structure is produced.
8. Elimination of central cores.
9. Adopted for mass production.

In order to take the above advantages of centrifugal casting process in the manufacturing of axis-symmetric parts i.e. cylinder liners, pipes, tubes etc., it is beneficial to model the process, and perform the simulation before manufacturing. In this report the simulation of solidification process of true centrifugal casting is considered with certain assumption to reveal the process before manufacturing. Many researchers have studied the defects in centrifugal castings and thought that the defects must be related to the solidification process of the centrifugal casting, i.e. they

depends to a large extent, on the characteristics of solidification. So it is very important to reveal solidification process in order to understand and avoid those defects.

Solidification in centrifugal castings is basically a similar process to that occurring in static castings, i.e. is a change of state phenomena, the rate of which is governed by heat transfer, but there are super-imposed effects of the mechanical action [Howson, 1969]. The ideal representation of solidification behavior in a true centrifugal casting is to assume that crystal growth commences with the liquid metal in contact with the mould wall, and then proceeds right across the section until the last remaining liquid freezes uniformly at the inner surface, to leave a smooth bore free from shrinkage cavities. Since the solidification process is related to the heat transfer process, numerical simulation may be an effective method to find out temperature profiles.

1.2 Problem Definition

1.2.1 Motivation

In centrifugal casting, it is very difficult to determine the temperature distribution and solidification time by experimental techniques. Because of this, accurate data on solidification time during centrifugal casting of different materials is not available. Their estimation is a complex problem mainly because the moving particles disturb the temperature equilibrium. Due to liquid and solid region in the casting during solidification, there is difference in thermo-physical properties of different regions of casting during solidification.

From literature review, it is clear that major defects in centrifugal casting are related to the solidification process， and it is not easy to take the temperature measurement of rotating body; therefore it is difficult to estimate the locations and magnitude of defects. Therefore, it is desirable to estimate solidification time and the influence of other processing parameters on the solidification time and temperature distribution in centrifugal casting through alternate means. Since the solidification process is related to the heat transfer of the casting-mold-ambient system, numerical simulation may be

an effective method for evaluation. Mathematical modeling of the centrifugal casting process based on heat and mass transfer analysis can be a useful alternate methodology. Numerical solution of modeled equations using "Finite Difference Technique" has been attempted in the present study. The heat transfer coefficient between the cast-mold interfaces, thermo-physical properties of casting material, mold material , and coating layer, initial temperature of the molten metal, and preheat temperature of mold material are considered as basic parameters, affecting solidification process and temperature distribution. A computer program for the solidification modeling of centrifugal casting can assist the foundries to predict the solidification time and temperature distribution of casting during solidification.

1.2.2 Objectives

- To understand the physics of the solidification process of centrifugal casting.
- To identify the various factors affecting solidification process of centrifugal castings.
- To study the inter-relationship of these parameters and their relative influence on the solidification process of centrifugal castings.
- To develop a mathematical model to determine the temperature distribution during solidification, and solidification time of centrifugal casting.
- Finally to implement and test the mathematical model in a computer program.

1.2.3 Approach

- Literature survey had been carried out to understand the physics of the centrifugal casting process.
- Based on the literature, various factors affecting the solidification process of centrifugal casting had been identified to make the model more realistic.
- Since the solidification process of casting is moving boundary problem, so various methods to solve the moving boundary problems had been studied.
- Suitable methods for mathematical modeling of solidification process of centrifugal casting had been identified based on the heat transfer equation.

- Solution procedure had been developed for the developed mathematical model of the process, based on the finite difference method.
- Computer program had been written to simulate the process and to analyze the effect of various factors on the process, and finally the developed program was validated against results available in literature, and results obtained from Ansys.

1.2.4 Organization of Report

- The chapter 2 gives the information about the literature survey carried out during the period of project.
- The chapter 3 deals with the mathematical formulation of solidification process of centrifugal casting.
- The chapter 4 deals with solution procedure adopted to solve the developed mathematical models.
- In chapter 5 results obtained through programming have been shown.
- The final chapter deals with the conclusions, which includes contribution, limitation and future scope of the project.

Chapter-2

Literature Review

2.1 Mode of Solidification

Solidification in centrifugal castings is a similar process to that occurring in static castings i.e. is a change of state phenomena, the rate of which is governed by heat transfer, but there are super-imposed effects of the mechanical action [Howson, 1969]. The ideal representation of solidification behavior in a true centrifugal casting is to assume that crystal growth commences with the liquid metal in contact with the mould wall, and then proceeds right across the section until the last remaining liquid freezes uniformly at the inner surface, to leave a smooth bore free from shrinkage cavities [Cumberland, 1963]. In this conception, the solidification front moves steadily towards the bore surface while feeding occurs progressively, solidification contraction being counteracted by liquid flowing outwards from the annular reservoir of molten metal at the bore. For this to happen there must be continuous flow of heat outwards, through the mould wall, to dissipate the latent heat of solidification, while the metal at the innermost surface remains molten until the liquid-solid interface has moved right up to the bore. In practice there is always a tendency for a certain amount of cooling to occur in the liquid metal at the bore during the time required for heat flow through the mold wall, so that the metal at the inner surface may reach its freezing point before the solidification front can cross the full section. If this occurs, then the last remaining liquid freezes in the annular zone between the main solidified mass and the minor growth from the bore, to leave a zone containing shrinkage cavities analogous to the center-line shrinkage characteristics of improperly fed plate castings.

The depth or position, at which this ‘center-line’ effect occurs, is essentially a function of the thermal conditions obtained during solidification. On the other hand, the severity of the shrinkage cavities in this zone is governed by the solidification contraction and freezing behavior of the alloy concerned.

The solidification behavior of cylindrical casting made by centrifugal casting and static casting is shown in the following figure to compare the casting soundness.

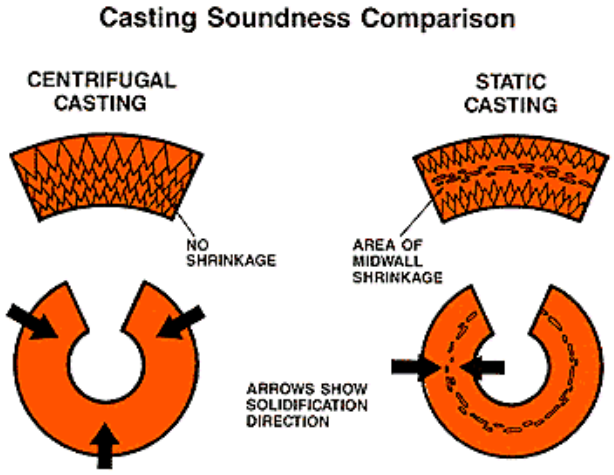

Fig 2.1. Solidification in centrifugal and static casting

2.1.1Factors affecting the solidification [Cumberland, 1963]

- Die temperature, die mass, thermal conductivity, specific heat, characteristics of any surface dressing, and the use of external cooling all are variables to determine how quickly solidification will occur from the outside surface.
- The temperature of molten metal entering the mould and the rate at which the liquid bath builds up are important in determining whether or not freezing will occur to an appreciable depth from the bore.

2.2 Factors affecting Centrifugal Casting [Jones, 1970, Janco, 1988]

1. Metal Composition and physical Properties

- Fluidity and density of metal.
- Chemical composition differences between start and completion of solidification.

- Temperature and the extent of the temperature differences between the start and completion of solidification, i.e. solidification range.

2. Casting Size:

- Diameter, wall thickness, and length.
- Relation of mass of metal to cooling surface.

3. Mold Material:

- Heat capacity and conductivity of mold.
- Mechanical properties of mold, especially at high temperatures.
- Properties and mold coating.

4. Casting Process

- Spinning speed of mold.
- Pouring temperature of metal.
- Pouring rate.
- Mold temperature, and cooling conditions.

2.3 Major Defects in Centrifugal Castings

Segregation Banding: Bands are annular zones of segregated, low-melting-point constituents, such as eutectic phases and oxide or sulfide inclusions [Janco, 1988]. Most alloys are susceptible to banding, but the wider the solidification range and the greater the solidification shrinkage, the more pronounced the effects may be.

Raining: In horizontal machine, if the mold is rotated at too low a speed or the metal poured into the mold too fast, raining occurs; that is, the molten metal actually rains or falls from the top of the mold to the bottom. It occurs because the molten metal has not been accelerated to the speed of rotation of the mold. If the friction of the molten metal against the mold wall is low, due to too slow a spinning speed, the molten metal will not reach a high enough rotative velocity to overcome the force of gravity and will fall off from the top of mold.

Shrinkage Cavities: When the metal is introduced into the mold rapidly, the degree of superheat is important. Excessive metal temperature slows solidification from the outside diameter more than it delays solidification from the bore and gives the worst conditions for the formation of deep shrinkage cavities.

Cold Shuts (laps): Cold shuts are caused by improper pouring techniques; irregular coverage of the mold surface produced by cold metal, turbulent pouring, interrupted or excessively slow pouring.

Pinholes (Gas holes, Blowholes): Few pinholes occur in centrifugally cast pipes, since they solidify under the influence of centrifugal force. However when liquid metal contains a large amount of gas, or the moisture content in the mold and the coating is not properly controlled, pinholes and blowholes will occur. These defects occur in metal molds because the metal casing does not have porosity for the gas to escape and the solidification rate of the metal is high.

Misrun and Liquid Interfaces: The major causes for such defects are too low casting temperature, too low pouring rate, and too high speed of rotation during casting.

Other defects: Sand and slag inclusions, penetration and dips, hot tears, inside surface shrinkage and cracks, operational cracks, and circumferential cracks are other defects generally occurred in centrifugal casting.

Some of the major troubles encountered may be avoided by paying careful attention to the variables listed above. But most of these defects are related to solidification process. We can find location and magnitude of these defects, if we know the solidification behavior of casting, and temperature distribution in casting during solidification of casting. Since the solidification process is related to the heat transfer of the casting-mold-ambient system, numerical simulation may be an effective method for evaluation. Some of the models related to solidification process of centrifugal casting available in literature had been studied and discussed in the next section.

2.4 Numerical Simulation

Computer Simulation of casting solidification is playing a significant role, as an important aspect of the integrated application of computers in the foundry industry. This technique of computer simulation offers a basis for predicting solidification patterns and parameters with greater accuracy, efficiency and economy both in time and money than empirical methods provided that both numerical methods and thermal

properties are suitably applied. Commercially available simulators are limited to the general problems of structural mechanics and heat transfer and are expensive and difficult to use. Hence there is need to develop centrifugal casting simulation for solidification process. Thus the developed software will assist the foundries to predict the solidification behavior of centrifugal castings.

2.4.1 Need of Numerical Simulation

Many researchers have studied the defects in centrifugal castings and thought that the defects must be related to the solidification process of the centrifugal casting, i.e. they depends to a large extent, on the characteristics of solidification. So it is very important to reveal solidification process in order to understand and avoid those defects. The temperature measurement of rotating body is not easy by experimental means; therefore it is difficult to estimate the locations and magnitude of defects. Since the solidification process relates to the heat transfer of the casting-mold-ambient system, numerical simulation may be an effective method for evaluation.

2.4.2 Architecture of Solidification modeling

An overall architecture of solidification modeling system is shown in fig3.1 [Upadhya et al, 1994]. Typical inputs for solidification simulation include properties of material (metal and mold), boundary conditions depending on the process and rigging design (which is based on initial design and empirical rules). Solidification simulation program calculates the time dependent temperature distribution, solid fraction, etc. inside the casting. The postprocessor takes inputs from simulated result and provides different result like grain size, dendrite arm spacing, macro and micro porosity, mushy zone formed and shrinkage stress distribution.

2.4.3 Basic Steps [Marrone, 1970]

Numerical simulation of solidification process requires following steps:

- Formulating an accurate physical description of the solidification process of casting in the mathematical form.

- Use of correct values for thermal properties of the materials involved.
- Performing a suitable numerical analysis (either FEM or FDM based) to obtain temperature relationships at specified space co-ordinates in the casting and mold.
- Post processing based on the simulated results to obtain the desired outputs.

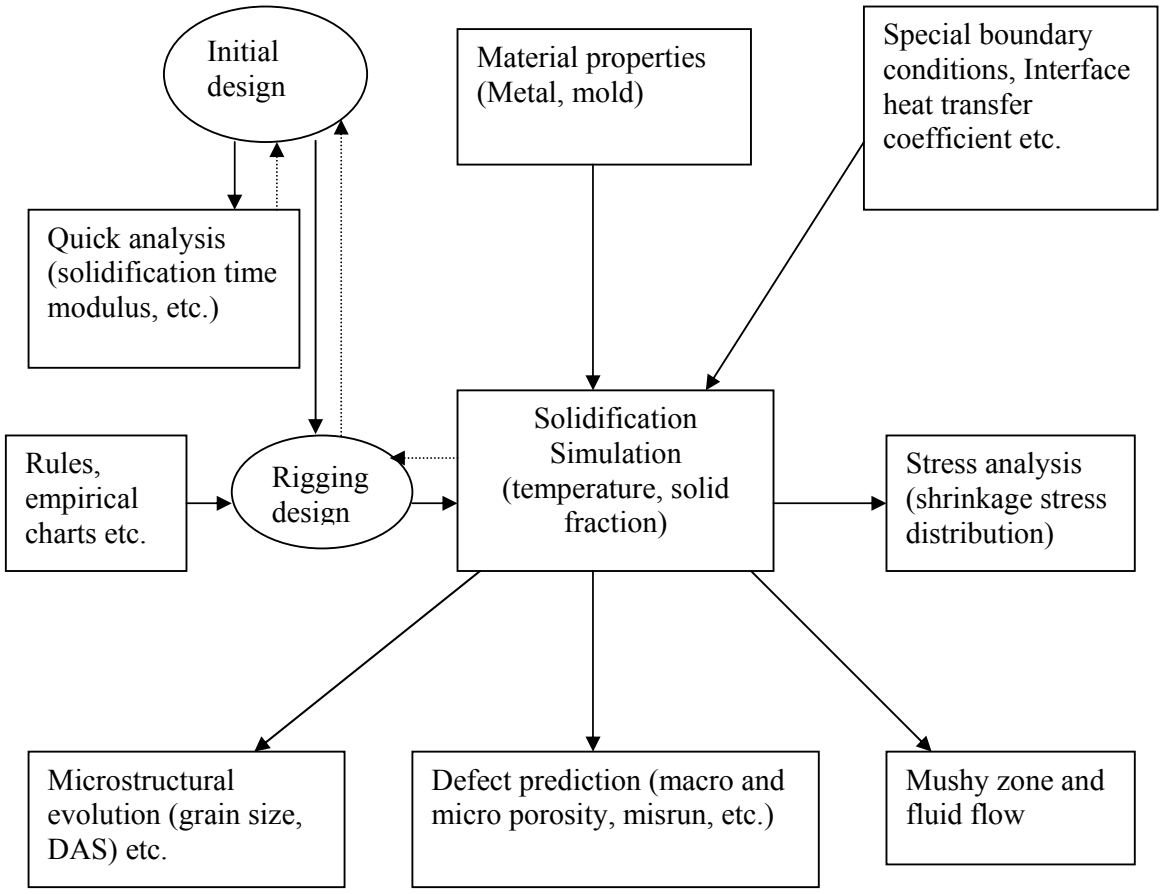

Fig 2.2. Architecture of a solidification modeling system [Upadhya et al, 1994]

2.4.4 Advantages of Numerical Simulation

- Increased yield of casting.
- Reduction in scrap and rework.
- Reduction in total manufacturing cost.
- Reduction in lead time.
- Improved quality of casting.
- Quick assessments in daily use.
- Highly visual results for easier communication with customer.
- Customer satisfaction.

2.5 Methods of Mathematical Formulation

The important feature of the phenomenon of solidification of casting is that it is brought by a process of heat transfer that is accompanied by a change of phase i.e. from liquid to solid. During a phase change, thermal energy is released or absorbed at the interface between the solid and the liquid. This energy, which is also known as latent heat of fusion, is drawn from one phase and distributed through the other by conductive or convective heat transfer.

The transfer of heat by conduction results from temperature difference within each phase, the release or absorption of the latent heat at interface occurs practically without any temperature difference. This characteristic of latent heat makes the phenomenon of solidification and melting a transient one.

In order to understand the process of solidification in castings one needs to know the rate of solidification, and should be able to calculate:

- The rate of heat transfer in materials undergoing solidification and melting.
- The rate of interface movement (or interface velocity) which yields the estimation of total solidification time in the materials of finite volume.
- The shape of interface at any instant of time.

2.5.1 Domain of Interest

It includes a region bounded by boundary (B) and occupied by a pure substance fig.2.3. At some instant of time, the solid (S) and liquid (L) phases are separated by an interface (I). The latent heat is absorbed or released at the interface, which is at fixed temperature T_f. Due to heat interaction at boundary (B), the interface moves through the domain with a velocity v_I. Equations of conservation of energy, mass and momentum are applied to small control volume within each phase and at the interface. When applying these equations two approaches are reported in the literature [Basu et al, 1988].

- Variable domain method, and
- Fixed domain method.

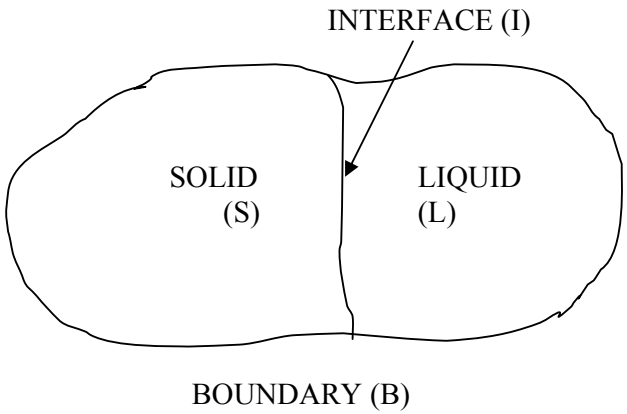

Fig 2.3. Domain of interest for pure metal

The essential difference between the two is that, in the former the total domain is divided into two phases and the interface region; and each region is treated separately. Since the volume of each region changes with time, the method is termed as variable domain method.

The second method considers the entire domain including all regions together; and since the total domain does not change with time, the method is termed as Fixed domain method.

Both methods have their advantages and disadvantages. It is obvious that in the Variable domain method the interface location is explicitly identified a priori whereas in the Fixed domain method the interface location is inferred from the solution of the governing equations.

2.5.2 Basic Equations

Solidification and melting being a thermo-fluid dynamic process, the application of laws of conservation of mass, momentum and energy to the control volumes situated in each phase yields partial differential equations governing the distribution of temperature (T), three velocity components (u,v,w) and pressure (P). The equations require information on material properties such as density (ρ) and specific heat (C_p), in addition to the transport properties such as kinematic viscosity (υ) and thermal diffusivity (α).

The equation for any dependent variable can be written in a generalized form as follows:

$$\frac{\partial}{\partial t}(\rho\psi) + div(\rho u\psi) = div(\Gamma grad\psi) + S \quad \text{..... (2.1)}$$

Table provides the value of Γ and S for different ψ's.

Table 2.1 Values of ψ, Γ and S in conservation equations

Ψ	Γ	S
u, v, w	$\mu = \rho.\nu$	$\partial p/\partial \eta + F_b$
T	$k/C_p = \rho\ \alpha$	$(\psi_{visc} + R_T)/C_p$
1	1	0

The last mentioned entry in table (i. e. $\psi = 1$) is the continuity equation applicable to a liquid phase. It enables determination of pressure distribution. In solid phase of course $u = S_{u,v,w} = 0$.

In the case of centrifugal casting convection effect is neglected and the only energy equation is considered with initial and boundary condition.

2.5.3 Boundary and Initial conditions

Solidification and melting being a transient phenomena, initial conditions must be specified for solution of equations along with the boundary conditions.

At commencement of solidification of liquid, the temperature can be assumed to be uniform and known both in casting as well as in mold region. The initial temperature in casting region may be equal to the pouring temperature T_p, and in mold region may be equal to mold preheat temperature.

The boundary conditions however require careful consideration in different applications. Hence each boundary condition is considered separately.

Boundary Condition

The most frequently encountered boundary condition for temperature is that of an energy flux q_b. Either the flux is specified at boundary or must be inferred from the temperature of the boundary, T_b and its environment, T_a. Thus for heating and cooling flux,

$$-k_{s,l}\left.\frac{\partial T}{\partial n}\right|_b = q_b(s) = h(s)\left(T_b - T_a\right) + \varepsilon_R \sigma\left(T_b^4 - T_a^4\right) \quad \text{..... (2.2)}$$

where s is distance along the boundary.

In most of the applications $q_b(s)$ is not specified but energy transfer takes place by convection and radiation, or by convection alone. The boundary condition is obtained by equating the heat conduction at boundary with the specified heat flux at boundary or heat transfer by convection and radiation from boundary to surrounding. Often zero flux boundary condition can be employed on a part of the boundary where adiabatic conditions prevail (e.g. symmetry planes and insulated surfaces).

Interface condition

In most application the interface movement rate is sufficiently low for equilibrium conditions to prevail at the interface. Thus two types of conditions are invoked at the interface,

- Equilibrium condition,
- Energy flux condition.

Equilibrium conditions

For pure substances, the interface is an isothermal surface with temperature equal to T_f.

$$T_l = T_s = T_f \quad \text{..... (2.3)}$$

Flux condition

A separate energy balance is required at the interface because of release or absorption of the latent heat during solidification or melting, respectively. The energy balance is as follows,

$$\left(k\frac{\partial T}{\partial n}\right)_l - \left(k\frac{\partial T}{\partial n}\right)_s = -\rho \Delta H v_I \quad \text{..... (2.4)}$$

2.5.4 Fixed domain method

The energy equation

In variable domain the transport of sensible heat in the two phases and that of latent heat at the interface were treated separately; these transport rates, however, were balanced by the conduction heat transfer rate (and source if any). Both the latent and the sensible heat contribute to changes in enthalpy. Use of enthalpy rather than the temperature, thus offers an opportunity for treating the two phases as well as the interface in a unified way. Thus irrespective of region being considered, the energy transfer is governed by the following equation,

$$\frac{\partial}{\partial t}(\rho H) + div(\rho u H) = div(k * gradT) \quad \text{..... (2.5)}$$

An equation, which has two dependent variable; enthalpy H and temperature T, is obtained and a relationship between H and T is needed to solve equation (2.5) for the entire domain without specific reference to the phases and the interface region.

Fig 2.4 shows that typical relationship between H and T is simply linear; the difficulty however arises at the interface. Several authors have proposed different H-T relationship for pure metals, which are as follows.

a) Model 1 by Szekely and Themlis [Szekely, and Thermlis, 1970]

$$H_I = f(C_p T) \quad \text{..... (2.6)}$$

where f is continuous linear function of T which is assumed to vary over a small temperature intervals 2ε or $T_f - \varepsilon < T < T_f + \varepsilon$

B) Model 2 by Meyer [Meyer, 1964]

$$H_I = Cp_s T + \left(\frac{\Delta H}{2\varepsilon}\right)\left(T - T_f + \varepsilon\right) \quad \text{..... (2.7)}$$

$$H_I = Cp_{eff} T + \left(\frac{\Delta H}{2\varepsilon}\right)\left(\varepsilon - T_f\right) \quad \text{..... (2.8)}$$

with $T_f - \varepsilon < T < T_f + \varepsilon$,

and $Cp_{eff} = Cp_s + \left(\Delta H / 2\varepsilon\right)$

C) Model 3 by Bonacina, [Bonacina, 1973]

$$H_I = Cp_{eff} T \quad \text{..... (2.9)}$$

with $T_f - \varepsilon < T < T_f + \varepsilon$,

and $Cp_{eff} = \dfrac{\Delta H}{2\varepsilon}$

d) Model 4 by Shamsunder and Sparrow [Shamsunder, and Sparrow, 1975]

$$\left(1/V\right)\int_V H_I dV = \left(1/V\right)\int_V \left(CpT_f + \Delta H\right) dV \quad \text{..... (2.10)}$$

The first three models simply assume that melting takes place over a range of temperatures rather than at a fixed value of the temperature i.e. T_f.

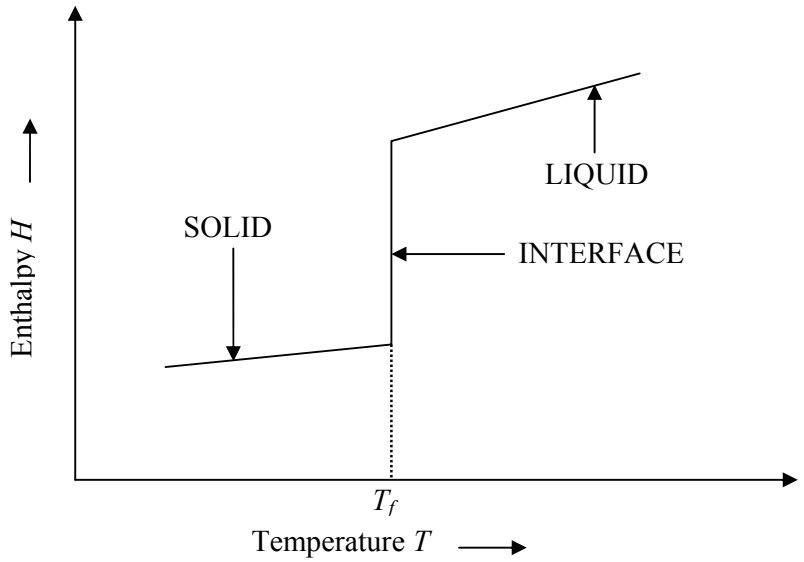

Fig 2.4 Enthalpy (H) and Temperature (T) relationship

Model 1 and 3 are similar except that the later assumes linearity between H and T, whereas the former allows for a non-linear variation. Model 2 is similar to model 3 but linearity constant is different. Fig 2.5 shows graphical representation of the three models. It is to be noted that ε is very small; the variation of Cp in model 3 is very sharp and has a spike.

Unlike the first three models, model 4 assumes that melting takes place over a small control volume V rather than over a small range of temperature.

The derivatives of enthalpy take the following form in different regions.

Solid $$\frac{\partial H}{\partial t} = \frac{\partial \left(Cp_s T \right)}{\partial t} \quad \text{..... (2.11)}$$

Liquid $$\frac{\partial H}{\partial t} = \frac{\partial}{\partial t}\left(Cp_l T + \Delta H \right) \quad \text{..... (2.12)}$$

Interface

Model 1 $$\left.\frac{\partial H}{\partial t}\right|_I = \frac{\partial f}{\partial t}\cdot\frac{\partial T}{\partial t} \quad \text{..... (2.13)}$$

Model 2 & 3 $$\left.\frac{\partial H}{\partial t}\right|_I = \frac{\partial}{\partial t}\left(C_{eff}T\right) \quad \text{..... (2.14)}$$

Model 4 $$\frac{1}{V}\frac{\partial}{\partial t}\int_V HdV = \frac{1}{V}\int_V \frac{\partial H}{\partial t}dV + \frac{\Delta H}{V}\frac{\partial V}{\partial t} = \frac{1}{V}\int_V \frac{\partial}{\partial t}\left(CpT_f\right)dV + \frac{\partial f_1}{\partial t} \quad \text{..... (2.15)}$$

The above equations result from Leibniz's rule where f_1 is the liquid fraction.

Model 1, 2 and 3 thus allow replacement of H in equation (2.5), which can be solved by any discretization technique without specific reference to interface. The new empirical inputs however are the value of ε and $\partial f/\partial T$ function.

Model 2 and 4 can also be interpreted in another way, if it is argued that melting takes place not only over a finite-temperature range or a finite-volume., but also over a finite time interval Δt, then relationship between H and T for all regions can be written as,

$$H\left(x,y,z,t\right) = CpT\left(x,y,z,t\right) + Hps\left(t\right) \quad \text{..... (2.16)}$$

such that

$$\int_t^{t+\Delta t}\frac{dH_{ps}}{dt}dt = \Delta H \quad \text{..... (2.17)}$$

The term $H_{ps}(t)$ can now be interpreted as:

Model 2 $$H_{ps}\left(t\right) = \left(\frac{\Delta H}{2\varepsilon}\right)\left(T - T_f + \varepsilon\right) \quad \text{..... (2.18)}$$

Model 4 $$\frac{dH_{ps}}{dt} = \Delta H\frac{df_1}{dt} \quad \text{..... (2.19)}$$

If equation (2.16) is used, then replacement of H will yield a source term in the energy equation i.e. $dHps/dt$.

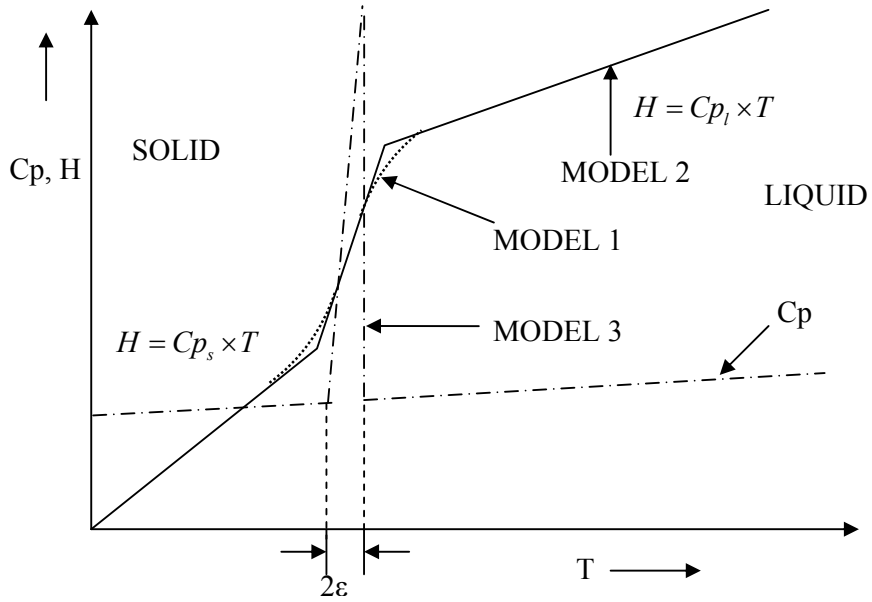

Fig 2.5. Approximation of H-T and Cp-T relationship

The equation can be solved without specifically locating the interface. Care is however needed in the choice of Δt when numerical solution over a discrete time steps is sought, so that equation is satisfied. In model 2 correct choices of Δt and ε must be made. Any arbitrariness in the choice of ε would result in an errorneous solution.

The models presented above are relatively simple when numerical solutions are sought over discrete time and space intervals. Although convenient to use, it is often found that the enthalpy models provide solutions that are at variance with exact solutions.

2.5.5 Variable domain methods

The energy conservation equation is derived with temperature as the dependent variable. The energy equation is solved in two regions (S and L) separately through energy balance at the interface. Location of the interface is the major problem, which is solved in all methods based on Variable domain formulations.

There are five different approaches for solving the phase change problem depending on the way of handling the interface. In Fixed grid method, a special differencing scheme is written near the interface. Either grid size or the number of grids is adjusted near the interface, so that the interface lies either on a grid point or on a line, in method of variable space grid. In the variable time step method the time step is selected such that the interface moves one grid per time step. In boundary immobilization method the interface remains fixed by transformation of co-ordinates. The isotherm migration method consists of exchanging one of the spatial co-ordinates with temperature, making the former a dependent variable.

2.5.5a Method of fixed grids

The usual way of solving the heat transfer equation over a fixed domain in one-dimension by a finite difference method is to evaluate the temperature at the discrete grid points on a fixed grid at different times. The complication associated with moving boundary arises at time, when the moving boundary (i.e. the interface) is located between two neighboring grid points, (iΔX) and (i+1) ΔX. In this method a special finite difference scheme based on unequal grid space interval is written near interface.

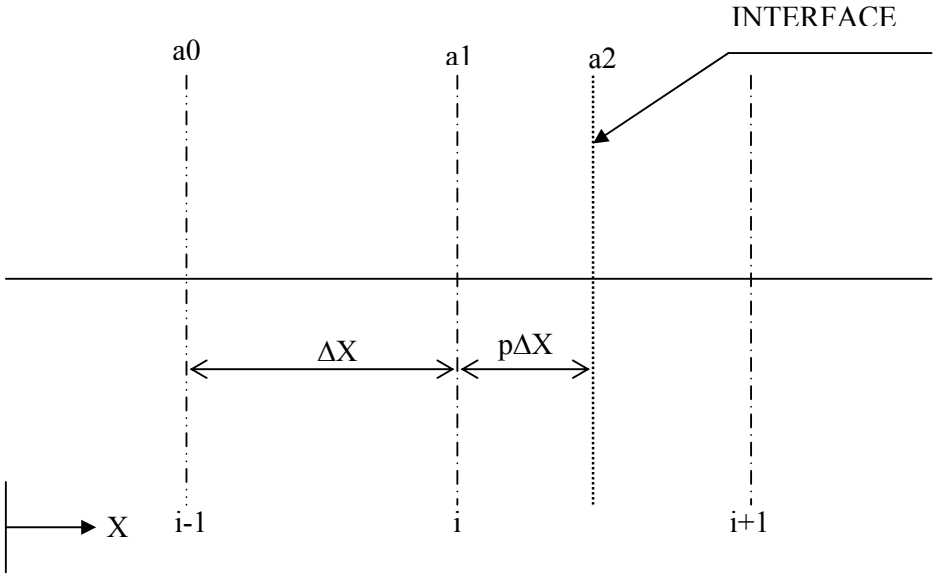

Fig 2.6. Grid arrangement for the method of Fixed Grids

It is assumed that the interface is located at a distance pΔX from the grid point (iΔX) at time t, using Langragian interpolation between the points a_0, a_1 and a_2 fig. 2.7 the space derivatives can be written as follows for X <I(t)

$$\frac{\partial^2\theta}{\partial X^2} = \frac{2}{\Delta X^2}\left(\frac{\theta_{i-1}}{p+1} - \frac{\theta_i}{p}\right), \qquad \text{at X = (iΔX)} \quad (2.20)$$

$$\frac{\partial\theta}{\partial X} = \frac{1}{X}\left(\frac{p\theta_{i-1}}{p+1} - \frac{p+1}{p}\theta_i\right), \qquad \text{at X = I (t)} \quad (2.21)$$

[Both equation (2.20) and (2.21) are written with $\theta_{interface}=0$, which follows from definition of θ]

Similarly for X > I (t), the interface energy balance equation takes the following form in one dimension.

$$\left(k\frac{\partial\theta}{\partial X}\right)_l - \left(\frac{\partial\theta}{\partial X}\right)_s = -\frac{\mathrm{Re}\,\mathrm{Pr}}{Ste}\rho^*\upsilon_I^* \quad (2.22)$$

Lazardis [Lazardis, 1970] used this method in multidimensional problems.

2.5.5b Method of variable space grids

In this method, the number of space intervals is kept constant and the space interval is a function of time. Differentiating temperature partially with respect to time one obtains the following equation instead of at constant *X*,

$$\frac{\partial\theta}{\partial t} = \left.\frac{\partial\theta}{\partial X}\right|_I \cdot \frac{\partial X}{\partial t} + \left.\frac{\partial X}{\partial t}\right|_X \quad (2.23)$$

A general grid point (*Xi*) moves according to the following relationship

$$\frac{dXi}{dt} = \frac{Xi}{I(t)} \cdot \frac{dI}{dt} \quad (2.24)$$

Hence for one dimensional problem, the governing equations will be modified for the variable space grids method as follows,

$$\frac{\partial\theta}{\partial t} = \frac{-Xi}{I(t)} \cdot \frac{dI}{dt} \cdot \frac{\partial\theta}{\partial X} + \frac{\partial^2\theta}{\partial X^2} \quad (2.25)$$

2.5.5c Method of variable time grid

In this method, the time step is calculated in such a manner that the interface moves one grid spacing per time step. For one dimensional problem it can be described as

$$\frac{\partial \theta}{\partial t} = \frac{\partial^2 \theta}{\partial X^2};\ 0 >= X >= I(t) \quad \text{..... (2.26)}$$

and the corresponding boundary conditions are

$$\frac{-\partial \theta}{\partial X} = Q\theta + R; \qquad X=0,\ t > 0 \quad \text{..... (2.27)}$$

$$\theta = 0; \qquad I(t) <= X <= 1.0,\ t>0 \quad \text{..... (2.28)}$$

$$\rho^* \operatorname{Re}\operatorname{Pr}\left(\frac{dX}{dt}\right) = Ste\left(\frac{\partial \theta}{\partial X}\right); \qquad X = I(t),\ t>0 \quad \text{..... (2.29)}$$

$$I(0) = 0 \quad \text{..... (2.30)}$$

Integrating equation (2.26) over X from 0 to I and using boundary conditions, the following integral equation results

$$Q\int_0^t \theta dt + Rt = \frac{\operatorname{Re}\operatorname{Pr}\rho^{*I(t)}}{Ste} - \int_0^{I(t)} \theta dX \quad \text{..... (2.31)}$$

with an initial guess of $\Delta t^{(0)}$, the finite difference form of equation (2.26) can be solved for the corresponding boundary and initial conditions, If the interface position is ($i\Delta X$) at the old time-level then the interface should be at $(i+1)\Delta X$ after the current time level. Substituting $I(t)$ by $(i+1)\,\Delta X$ along with the new temperature solution, one can obtain a new time step, $\Delta t^{(1)}$, from equation (2.31). If $\Delta t^{(0)}$ and $\Delta t^{(1)}$ match, then $\Delta t^{(1)}$ is the required time step. Otherwise, the iteration is continued till $\Delta t^{(k)}$ and $\Delta t^{(k+1)}$ match to certain accuracy. Gupta and Kumar [Gupta, and Kumar, 1981] used the generalized boundary condition to solve one dimensional problem.

2.5.5d Boundary immobilization method

This is the most powerful method in Variable domain method formulation, Finite difference methods are more straight forward in application to the problems governed by non-linear partial-differential equations in a fixed region than for linear equations in a changing domain. Hence, the space variable is transformed in the boundary immobilization method in order to fix the moving interface. With this transformation,

the governing equations which are linear become non-linear partial-differential equations.

For a one dimensional problem, using the transformation $\xi = X / I(t)$, the governing equation takes the following form

$$I^2\left(\frac{\partial\theta}{\partial t}\right) - \xi I\left(\frac{dI}{dt}\right)\cdot\left(\frac{\partial\theta}{\partial\xi}\right) = \left(\frac{\partial^2\theta}{\partial\xi^2}\right) \quad \text{..... (2.32)}$$

The second term on the left hand side is similar to the convective term. The control volumes (or grid points) are stationary in the transformed plane (ξ,t), but they move in the physical plane (X,t) and this results in a convective flux in the transformed governing equation. This term can be called the "pseudo-convection" term. In multi-dimensional problem, there are some more cross derivatives in the final differential equation other than the pseudo-convective terms.

2.5.5e Isotherm migration method

In this method, the heat flow equation is written in a form which concentrates attention on the movement of isotherms. Temperature is exchanged with one of the space variables making temperature an independent variable. In one dimension the governing equation takes the form,

$$\frac{\partial X}{\partial t} = \left(\frac{\partial X}{\partial\theta}\right)^{-2}\left(\frac{\partial^2 X}{\partial\theta^2}\right) \quad \text{..... (2.33)}$$

This equation for any boundary conditions can be solved by any standard finite difference method. Crank and Gupta [Crank, and Gupta, 1975] used this method to solve a two dimensional solidification problem of a saturated liquid in an infinitely long square prism. Crank and Crowley [Crank, and Crowley, 1978] suggested a novel way of implementing the isotherm migration method, using the fact that heat flow will always be normal to isotherm, they wrote the governing equation in terms of a local co-ordinate treating the isotherm element as part of a cylindrical system.

In the next chapter the mathematical model has been formulated for the solidification process of centrifugal casting using both Fixed domain method and Variable domain method.

Chapter-3

Mathematical Modeling

The mathematical model has been formulated, essentially based on heat transfer and solidification consideration of centrifugal casting. A schematic representation of the model of the centrifugal casting is shown in fig 3.1. The heat is withdrawn from the liquid region of the casting (which is initially at pouring temperature) to the metallic mold (which is at initial preheat temperature), and finally from mold to surrounding. Heat is also radiated away from the inner surface of the casting. As the solidification proceeds by conductive heat transfer through the molten metal in contact with metallic mold, the solid-liquid interface moves away from the metallic mold.

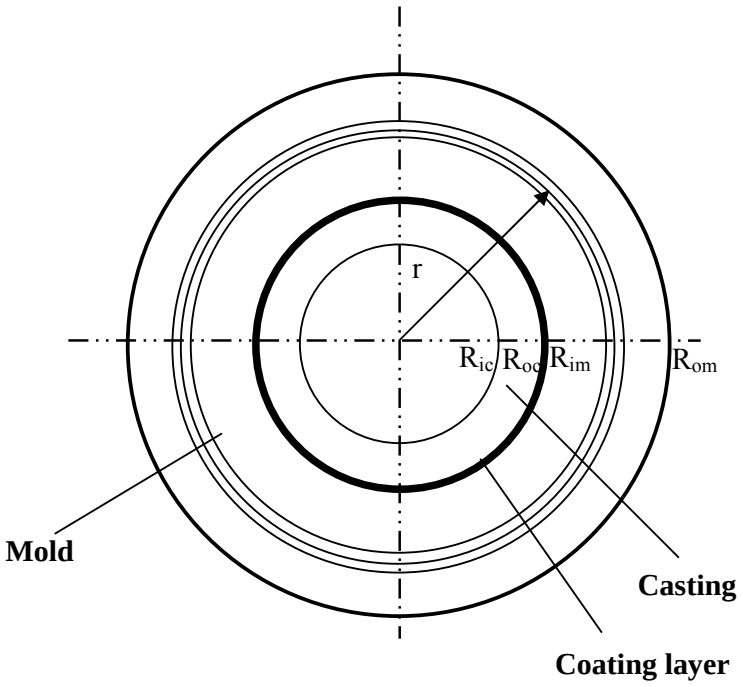

Fig3.1. Geometry of horizontal-axis centrifugal casting

3.1 Model Formulation

The principal model equations are heat transfer equations for various regions comprising the process. The model is based on the following assumptions:

- The heat flow is purely one dimensional and perpendicular to the mold wall.
- The mold is filled with liquid metal instantaneously.
- No fluid flow during solidification.
- The interface position between solid and liquid regions is calculated by assuming it to be planar.
- Heat transfer between casting and mold is assumed by means of conduction, whose efficiency decreases as solidification progresses as the function of solidification thickness.

3.2 Heat Conduction Formulation

The heat transfer in various regions of casting (liquid melt, solidified casting region) and mold is governed by one dimensional unsteady state heat conduction equation written in cylindrical co-ordinates.

$$\frac{\partial T_i}{\partial t} = \frac{1}{C_i \rho_i} \{ \frac{\partial}{\partial r} (k_i \frac{\partial T_i}{\partial r}) + \frac{k_i}{r} . \frac{\partial T_i}{\partial r} \} \quad \text{..... (3.1)}$$

Where $i = l, s, m$ for the liquid region, solid region and steel mold region, respectively.

Since the thermal conductivity k and C varies with temperature (density ρ is assumed constant), while solving with Explicit finite difference method to take into account, this variation of thermal conductivity k, a function ϕ is introduced, which is expressed in terms of [Ebisu, 1977]

$$\phi = \int_{Td}^{T} \frac{k}{k_d} dT \quad \text{..... (3.2)}$$

Where T_d is known temperature and k_d is thermal conductivity at that temperature. The equation (3.1) can be written in the form of ϕ as

$$\frac{\partial \phi}{\partial t} = \frac{k}{C\rho}\{\frac{\partial}{\partial r}(\frac{\partial \phi}{\partial r}) + \frac{1}{r}.\frac{\partial \phi}{\partial r}\} \quad \text{..... (3.3)}$$

To take into account of variation of specific heat with temperature, we can write specific heat and temperature in term of heat content H as

$$\frac{\partial H}{\partial T} = C \quad \text{..... (3.4)}$$

Substituting the relations $\frac{\partial H}{\partial T} = C$, $\frac{\partial \phi}{\partial T} = \frac{k}{k_d}$ and $\frac{\partial H}{\partial T} = \frac{\partial H}{\partial t}.\frac{\partial t}{\partial T}$ into equation (3.3)

$$\frac{\partial H}{\partial t} = \frac{k_d}{\rho}\{\frac{\partial}{\partial r}(\frac{\partial \phi}{\partial r}) + \frac{1}{r}.\frac{\partial \phi}{\partial r}\} \quad \text{..... (3.5)}$$

3.3 Initial Condition

During centrifugal casting, before pouring the molten metal (which is at temperature T_p) into the mold, the mold is preheated to a certain temperature (T_M) to avoid the thermal damage to the mold. Therefore the initial temperature (at time $t=0$) in the casting and mold regions considered as

$$T_c = T_p \quad \text{..... (3.6)}$$

$$T_m = T_M \quad \text{..... (3.7)}$$

As soon as the liquid metal comes in contact with the mold wall, the temperature of the metal-mold interface increases suddenly. The initial interface temperature can be approximated by considering the thermal energy conservation within the very thin layer of the metal and the mold in adiabatic system [Ebisu, 1977, Phelke et al, 1978]. Since the heat flow rate from the metal to mold at the beginning is very rapid indeed, it can be stated that the liquid metal within this layer solidifies instantaneously.

In order to find the metal-coating layer interface temperature at time $t=0$, the mold is assumed to be at a temperature T_M and the initial temperature of casting is assumed to be the temperature of the metal as it enters the mold cavity. To find a reasonable approximation to the initial interface temperature, consider an adiabatic system shown in Fig 3.2.

The thermal energy initially contained in this system is $2\Pi R_{oc}\partial r\ (\rho_t C_t T_M + \rho_I C_I T_p)$. The system is allowed to come to equilibrium adiabatically. The adiabatic assumption is reasonable because as $\partial r \rightarrow 0$ whatever happens to the system, it is assumed to happen instantly. Also, by definition of this condition, no heat flux has yet been established, hence no heat is transferred to or from the system. Depending upon the relative values of $\rho_t, \rho_I, C_t, C_I, T_M, T_p$, and the heat of fusion of the metal (ΔH), there are three possible final states of system.

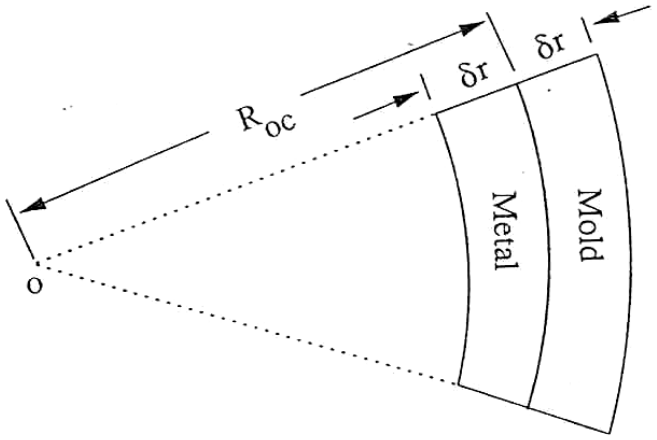

Fig 3.2. Control volume considered when calculating the initial temperature of metal-mold interface

Case 1: None of metal solidifies:

Equating the thermal energy in the system initially to that in the system at equilibrium yields

$$2\Pi R_{oc}\partial r\left(\rho_t C_t T_M + \rho_I C_I T_p\right) = 2\Pi R_{oc}\partial r\left(\rho_t C_t + \rho_I C_I\right)T_0$$

Where T_o is the initial metal-coating layer interface temperature. On rearranging the terms the interface temperature can be written as

$$T_0 = \frac{\rho_I C_I T_P + \rho_T C_T T_M}{\rho_I C_I + \rho_T C_T} \quad \text{..... (3.8)}$$

Case 2: All the metal solidifies:

The thermal energy released when metal solidifies is $2\Pi\ R_{oc}\partial r\ (\rho_I \Delta H)$

Conservation of energy yields

$$2\Pi R_{oc}\delta r(\rho_I C_I T_I + \rho_T C_T T_M) + 2\Pi R_{oc}\delta r(\rho_I \Delta H) = 2\Pi R_{oc}\delta r(\rho_I C_I + \rho_T C_T)T_0$$

On rearranging terms, T_o can be written as

$$T_0 = \frac{\rho_I C_I T_p + \rho_T C_T T_M + \rho_I \Delta H}{\rho_I C_I + \rho_T C_T} \quad \text{..... (3.9)}$$

Case 3: The metal partially solidifies:

If the liquidus and solidus lines of a binary system are approximated by straight lines, the fraction of liquid solidified as a function of temperature can be expressed as

$$FS = \frac{T_L - T}{T_L - T_f} \quad \text{..... (3.10)}$$

where T_L and T_f are the liquidus and solidification front temperatures, respectively. Equating thermal energy in the system initially to that in the system at equilibrium yields

$$2\pi R_{oc}\delta r[(\rho_T C_T T_M + \rho_I C_I T_p) + \rho_I \Delta H \frac{T_L - T}{T_L - T_f}] = 2\pi R_{oc}\delta r(\rho_T C_T + \rho_I C_I)T_o$$

On rearranging terms, T_o can be written as

$$T_0 = \frac{\rho_I C_I T_p + \rho_T C_T T_M + \frac{\rho_I \Delta H T_L}{T_L - T_f}}{\rho_I C_I + \rho_T C_T + \frac{\rho_I \Delta H}{T_L - T_f}} \quad \text{..... (3.11)}$$

It is necessary to assume the final state of the metal (liquid, mushy, or solid) in order to determine the initial interface temperature. After estimating T_o using the appropriate equation according to the assumed condition, its value is checked to ensure that the calculated T_o falls within the temperature range initially assumed.

3.4 Boundary Conditions

3.4.1 Outer surface of mold

At the outer surface of mold heat is transferred from mold to surrounding air by radiation and convection, but is mostly due to convection because lower temperature of mold at outer surface, which is given by:

$$w = \sigma F \varepsilon_M \{(\overline{T}_{r_3,t} + 273)^4 - (T_a + 273)^4\} + h_2(\overline{T}_{r_3,t} - T_a) \quad \text{..... (3.12)}$$

Where $\overline{T}_{r3,t}$ = surface temperature of mold.

F = configuration factor for radiation = 1 for cylinder.

ε_M = emissivity of mold

And due to conduction

$$w = -k_m \frac{\partial T_m}{\partial r} \quad \text{..... (3.13)}$$

By equating the above two equation the boundary temperature of mold can be calculated.

3.4.2 Inner surface of casting, i.e. at r= r1

At inner surface of casting the heat is transferred by convection and radiation, but since air is not moving at inner surface one can assume adiabatic boundary condition at inner surface of casting.

$$-k_I \frac{\partial T}{\partial r} = h_1(T_{ci} - T_\beta) + \sigma F \varepsilon_c \left\{ (T_{ci} + 273)^4 - (T_a + 273)^4 \right\} \quad \text{..... (3.14)}$$

3.4.3 At Ingot/ coating layer/ mold interfaces

Before air/gap formation

Heat is transferred by conduction until an air gap is formed between ingot and mold. The temperature at the ingot/coating layer interface can be determined using heat flux w

$$w = K \frac{T_{r_2,t} - \overline{T}_{r_2,t}}{d} \quad \text{..... (3.15)}$$

By using appropriately above equation in finite difference form we can calculate the interface temperature between ingot/coating layer and coating layer/mold interfaces.

After air/gap formation

As solidification proceeds, an air gap will form between ingot and mold because of the contraction of metal due to solidification and thermal expansion of mold.

If heat is transferred by radiation, the heat flux is given by:

$$w = const.\{(T_{r_2,t} + 273)^4 - (\overline{T}_{r_2,t} + 273)^4\} \quad \text{.....(3.16)}$$

It was more reasonable and was in good agreement with foundry experiences to state that the heat is transferred by conduction whose 'efficiency' decreases as solidification proceeds [Ebisu, 1977].

Therefore, the heat flux was assumed to exponentially decrease as given by Equation (3.17)

$$w' = w\exp(-\beta s(t)) = -K.\frac{T_{r_2,t} - \overline{T}_{r_2,t}}{d}.\exp(-\beta s(t)) \quad \text{..... (3.17)}$$

Where β = damping coefficient.

$s(t)$ = solidified thickness.

Thus consider Eq. (3.17) instead of Eq. (3.15) while solving the basic equation.

3.4.4 At solid-liquid interface, i.e., at r =$R_{s(t)}$

For pure metal at the solid-liquid interface the temperature of both regions will be equal to the freezing temperature.

$$T_{sc} = T_{lc} = T_f \quad \text{..... (3.18)}$$

3.4.5 The energy balance at solid-liquid interface, at r = $R_{s(t)}$

It is obtained by equating the rate of heat removed from the solid phase in the positive r direction to the sum of rate of heat supplied to the interface from the liquid phase in the positive r direction and rate of heat liberated at the interface during solidification, .

$$-k_{sc}\frac{\partial T_{sc}}{\partial r} = -k_{lc}\frac{\partial T_{lc}}{\partial r} + \rho_{sc}\Delta H\frac{\partial s(t)}{\partial t} \quad \text{..... (3.19)}$$

3.5 Problem Formulation in terms of dimensionless variables

Since the problem does not permit an exact solution, numerical solution techniques have been adopted, as these can provide results of assured accuracy. To facilitate solutions via a finite difference technique, it appears advantageous to work in a domain of unchanging size in which the grid can be fixed once and for all [Raju et al, 2000]. This requires that the moving boundary be immobilized by the transformation

of variables [Kang, and Rohatgi, 1996, Ramachandran et al, 1981, Saitoh, 1978]. This also serves to introduce dimensionless variables. For this a new co-ordinate system with origin at the outer surface of the casting is defined which is schematically shown in Fig. 3.3. The thickness of solidified front at given time is represented by s(t). The problem then is to find the time taken for the solid-liquid interface to move from $\bar{r} = 0$ to $\bar{r} = ri$.

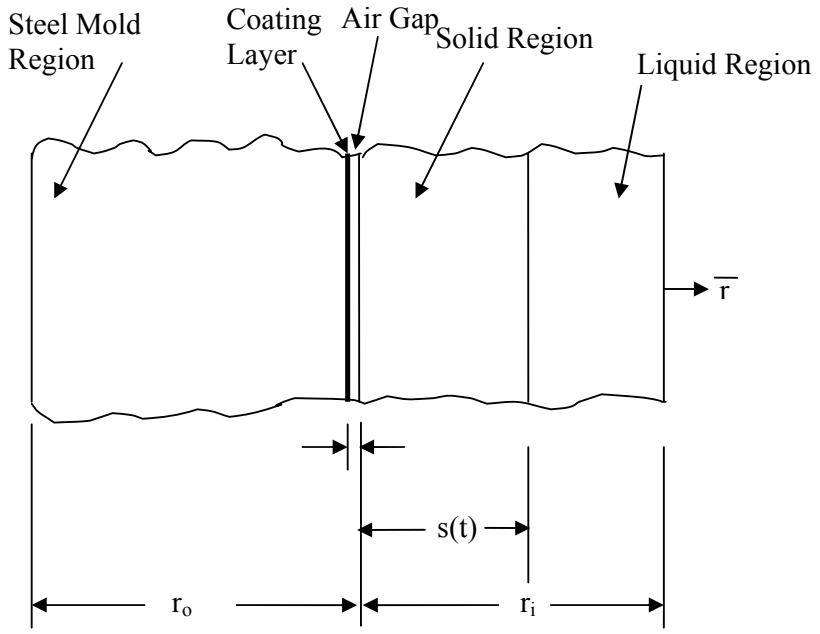

Fig 3.3. One dimensional model to find the temperature distribution and position of the solid-liquid interface

The new space co-ordinates in solid and liquid regions are defined as

$$\xi = \frac{\bar{r}}{s(t)} = \frac{R_{oc} - r}{s(t)} \qquad (0 \le \bar{r} \le s(t)) \qquad \text{(3.20)}$$

$$\eta = \frac{\bar{r} - s(t)}{r_i - s(t)} = \frac{R_{oc} - r - s(t)}{r_i - s(t)} \quad (s(t) \le \bar{r} \le r_i) \qquad \text{(3.21)}$$

so that $0 \le \xi \le 1$ and $0 \le \eta \le 1$ in the each region respectively for all the time. The transformation of the governing equations is facilitated by the following relations respectively for the solid and liquid regions

$$\frac{\partial}{\partial r} = \frac{-1}{s(t)} \frac{\partial}{\partial \xi}, \qquad \frac{\partial}{\partial t} = \frac{\partial}{\partial t} - \frac{\xi}{s(t)} \frac{ds(t)}{dt} \frac{\partial}{\partial \xi} \qquad \text{(3.22)}$$

$$\frac{\partial}{\partial r}=\frac{-1}{r_i-s(t)}\frac{\partial}{\partial \eta},\qquad \frac{\partial}{\partial t}=\frac{\partial}{\partial t}-\frac{(1-\eta)}{r_i-s(t)}\frac{ds(t)}{dt}\frac{\partial}{\partial \eta} \quad \text{..... (3.23)}$$

The additional terms in the transformation of terms in Equations (3.22) and (3.23), respectively, have an interesting physical interpretation. They represent convection associated with the immobilization of a moving boundary. An observer positioned on an immobilized moving boundary sees mass moving toward or away from him, and this mass is responsible for convection [Sparrow et al, 1978].

The transformation of governing equation (3.1) for solid region and the boundary conditions to the solid region, equations (3.17) and (3.18), are written as follows, respectively

$$\frac{\partial T_{sc}}{\partial t}=\frac{\alpha_{sc}}{s^2(t)}\frac{\partial^2 T_{sc}}{\partial \xi^2}+\left[\frac{\xi}{s(t)}\frac{ds(t)}{dt}-\frac{\alpha_{sc}}{R_{oc}-\xi s(t)}\frac{1}{s(t)}\right]\frac{\partial T_{sc}}{\partial \xi} \quad \text{..... (3.24)}$$

$$\text{at } \xi=0 \qquad \frac{k_{sc}}{s(t)}\frac{\partial T_{sc}}{\partial \xi}=\frac{K}{d}\left(T_{oc}-T_{im}\right)\times\exp\left(-\beta s(t)\right) \quad \text{..... (3.25)}$$

$$\text{at } \xi=1 \qquad T_{lc}=T_{sc}=T_f \quad \text{..... (3.26)}$$

Similarly for the liquid region ($0\le\eta\le 1$) the equation (3.1), and the boundary conditions represented by equations (3.18) and (3.14) are transformed, respectively, as

$$\frac{\partial T_{lc}}{\partial t}=\frac{1}{\left(r_i-s(t)\right)}\left[(1-\eta)\frac{ds(t)}{dt}-\frac{\alpha_{lc}}{\left(R_{oc}-s(t)\right)-\eta\left(r_i-s(t)\right)}\right]\frac{\partial T_{lc}}{\partial \eta}+\frac{\alpha_{lc}}{\left(r_i-s(t)\right)^2}\frac{\partial^2 T_{lc}}{\partial \eta^2} \quad \text{(3.27)}$$

$$\text{at } \eta=0 \qquad T_{lc}=T_{sc}=T_f \quad \text{..... (3.28)}$$

$$\text{at } \eta=1 \qquad \frac{-k_{lc}}{r_i-s(t)}\frac{\partial T_{lc}}{\partial \eta}=h_1\left(T_{ic}-T_{\beta}\right) \quad \text{..... (3.29)}$$

The energy balance equation at the solid-liquid interface can be rewritten as

$$\frac{\partial s(t)}{\partial t}=\frac{k_{sc}}{\Delta H\rho_{sc}}\left(\frac{1}{s(t)}\frac{\partial T_{sc}}{\partial \xi}-\frac{k_{lc}}{k_{sc}}\frac{1}{r_i-s(t)}\frac{\partial T_{lc}}{\partial \eta}\right) \quad \text{..... (3.30)}$$

Since there is no phase transformation in the two mold regions, equation (2.1) without transformation is used to calculate the mold temperatures.

The above-formulated mathematical model had been solved by both fixed domain and variable domain methods and the solution procedure for both methods is described in

next chapter. The equations presented in the first part of this chapter have been solved by enthalpy formulation using explicit finite difference method, in which temperature is converted into the heat content. Thus the solution of these equations have been obtained in term of enthalpy, the temperature is obtained from this enthalpy by suitable relation between temperature and enthalpy.

The equations developed in terms of dimensionless variables have been solved by boundary immobilization method using implicit variable time step scheme. The solution from these equations is directly obtained in term of the temperature in various regions. The detailed solution procedure has been explained in the next chapter.

Chapter-4

Solution Procedure

The modeled equations have been solved numerically by fixed domain method using simple explicit finite difference technique, in which temperature is written in term of the heat content. Then in order to locate the interface position explicitly equations developed in terms of dimensionless variables are solved by Variable domain method using implicit moving boundary immobilization method.

4.1 Fixed Domain Method

To solve the modeled equations the "*r*-*t*" domain is subdivided into small intervals of constant Δr_1 and Δr_2, for casting and mold respectively, in space, and Δt in time as shown in figure 4.1. For this a number of nodes were assumed in casting and mold regions, and corresponding Δr_1 and Δr_2 interval in space for casting and mold regions are calculated. Based upon stability criteria, for these step intervals, time step Δt was found out for different regions. Then minimum from these time intervals is taken as time step Δt for the whole domain.

4.1.1 Finite Difference Approximation

The differential equation and the boundary conditions for both the mold region and casting region can be discretized using explicit method with the forward in time and central in space finite difference scheme. In this method user inputs the number of nodes for both casting and mold region. After getting the number of nodes, each region is subdivided into the corresponding number of grids. After calculating Δr_1 and Δr_2 space increments in casting and mold region respectively, based upon stability criteria Δt has been calculated for different regions as per the basic equation and different boundary conditions. Now from these calculated time steps the minimum time step is chosen as time step for whole domain.

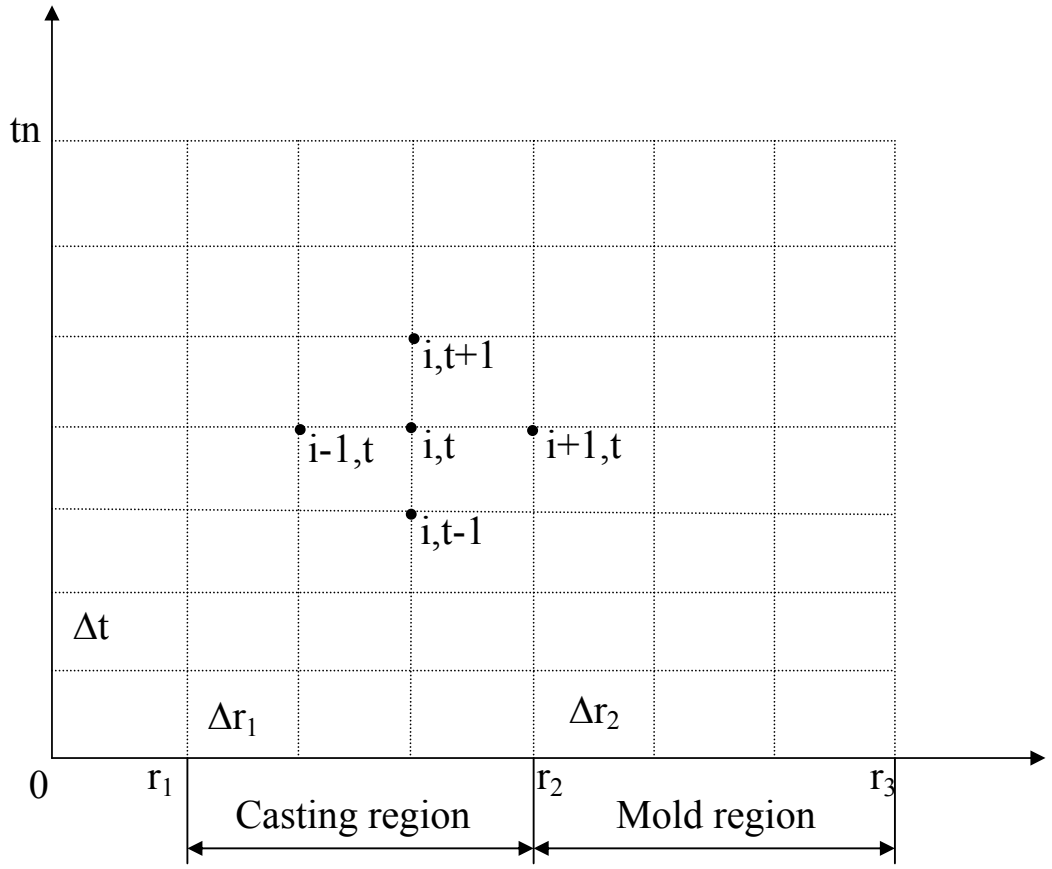

Fig4.1 Subdivision of "r-t" domain using Δr, and Δt

For forward difference in time and central difference in space the equation (3.1) can be written in the following finite difference form:

$$\frac{T_{i,t+1}-T_{i,t}}{\Delta t}=\frac{k}{C\rho}\{\frac{T_{i+1,t}-2T_{i,t}+T_{i-1,t}}{(\Delta r)^2}+\frac{T_{i+1,t}-T_{i-1,t}}{r*2\Delta r}\} \quad \text{..... (4.1)}$$

To take into account, the variation of thermal conductivity and specific heat of casting and mold material, from above equation and equations (3.2), (3.3), (3.4), the equation (3.5) can be written in the following form:

$$H_{r,t+1}=H_{r,t}+\frac{k_d\Delta t}{2r(\Delta r)^2\rho}[(2r+\Delta r)\phi_{r+1,t}-4r\phi_{r,t}+(2r-\Delta r)\phi_{r-1,t}] \quad \text{... (4.2)}$$

Where suffixes *r-1, r, r+1* are continuous nodal points in the radial direction and *t, t+1* continuous time. Since heat content *H* and function ϕ does not indicate temperature itself, it is necessary to correlate these to temperature. Therefore it is necessary to find out the correlation between *H-T* and ϕ *-T*. This can be found out if

we know the variation of thermal conductivity and specific heat with respect to temperature for both casting and mold material.

4.1.2 Boundary Temperatures

At outer surface of mold

To find out, the temperature at outer surface of mold in above equation we need the term $\phi_{r+1,t}$, which is missing. We can find out this term from equation (3.13)

$$w = k_m \frac{\partial T_m}{\partial r} = k_d(M) \frac{\phi_{r-1,t} - \phi'_{r+1,t}}{2\Delta r_2} \quad \text{..... (4.3)}$$

Thus $\phi'_{r+1,t}$ is determined from equation (4.3) and equation (3.12), and used instead of $\phi_{r+1,t}$ in equation (4.2) to calculate the boundary temperature at the outer surface of mold. Similar procedure is adopted to find out boundary temperature at inner surface of casting and Ingot/coating layer/mold interfaces.

4.1.3 Determination of time and size increments

Determination of time and size increments; i.e. distance between nodal points in the radial direction, is the key to the stability of the method. The criteria for the stability are driven from the finite difference equations as follows-

If number of nodes in casting region is n_1 and in mold region is n_2, then Δr_1 in casting region and Δr_2 in mold region is found out by following formulae:

$$\Delta r_1 = \frac{R_{oc} - R_{ic}}{n_1 - 1} \quad ; \text{And} \quad \Delta r_2 = \frac{R_{om} - R_{im}}{n_2 - 1} \quad \text{..... (4.4)}$$

Within ingot and mold

Requirement for stability is that the term influencing on the future temperature be positive physically, thus from equation (4.2)

$$\bar{H}_{r,t} - \frac{k_d(M)\Delta t}{r(\Delta r_2)^2 \rho_M} \{2r\bar{\phi}_{r,t} + \frac{(2r + r_2)}{k_d(M)} w\} \geq 0$$

Substituting the relation $\frac{\partial H}{\partial T} = C$, $\frac{\partial \phi}{\partial T} = \frac{k}{k_d}$ into the above equation yields

$$\Delta t \le \frac{1}{\frac{2k}{C\rho}.\frac{1}{(\Delta r)^2}} \quad \text{..... (4.5)}$$

Outer surface of mold

Since the temperature (or *H*) at outer surface of mold is expressed in the same manner as above equation, the criteria for the outer surface of mold is-

$$\bar{H}_{r,t} - \frac{k_d(M)\Delta t}{r(\Delta r_2)^2 \rho_M}\{2r\bar{\phi}_{r,t} + \frac{(2r+r_2)}{k_d(M)}w\} \ge 0$$

And

$$w = \sigma F \varepsilon_M \{(T_{r3,t}+273)^4 - (T_a+273)^4\} + h_2(T_{r3,t} - T_a)$$

or $$w = const.(T_{r3,t} - T_a) + h_2(T_{r3,t} - T_a)$$

Where

$$const. = \sigma \varepsilon_M F(T_{r3,t} + T_a - 576)\{(T_{r3,t}+273)^2 + (T_a+273)^2\}$$

Also,

$$\frac{\partial \bar{H}_{r,t}}{\partial T} = C_M$$

$$\frac{\partial \bar{\phi}_{r,t}}{\partial T} = \frac{k}{k_d(M)}$$

$$\frac{\partial w}{\partial T} = h_2 + const.$$

Substitution of these relations into the above inequality gives

$$\Delta t \le \frac{1}{\frac{2k_M}{C_M \rho_M}(\frac{1}{(\Delta r_2)^2} + \frac{h_2 + const.}{\Delta r_2 k_M})} \quad \text{..... (4.6)}$$

Ingot/coating layer interface

Similarly as driven in the above,

$$\Delta t \le \frac{1}{\frac{2k_I}{C_I \rho_I}(\frac{1}{(\Delta r_1)^2} + \frac{k}{\Delta r_1 k_I d})} \quad \text{..... (4.7)}$$

Mold/coating layer interface

Similarly,

$$\Delta t \le \frac{1}{\frac{2k_M}{C_M \rho_M}\left(\frac{1}{(\Delta r_2)^2} + \frac{k}{\Delta r_2 k_M d}\right)} \quad \text{..... (4.8)}$$

Thus the Δt has been calculated from above equations for different regions of casting and mold material. The minimum of these Δt is taken as time step for whole domain.

4.1.4 RELATIONS OF *H-T* AND *Φ-T* [8]

Equations for H-T relationship-

From $\frac{\partial H}{\partial T} = C$, $H = \int cdT + const.$ $H = \int cdT + const.$

The equations for H-T were determined using the data shown in fig 3.2 and fig 3.3

Thus, for low carbon steel –

0 to 200 ^{0}C: $H = 0.1175\ T$

200 to 300 ^{0}C: $H = 0.1300\ T\text{-}2.50$

300 to 400 ^{0}C: $H = 0.1395\ T\text{-}5.35$

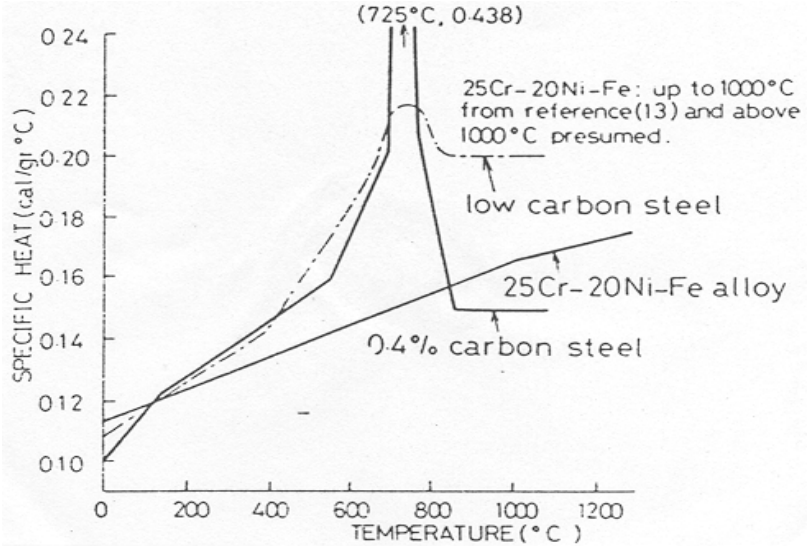

Fig 4.2 Specific heats of 25% Cr –20% Ni - Fe alloy and carbon steels [Ebisu, 1977]

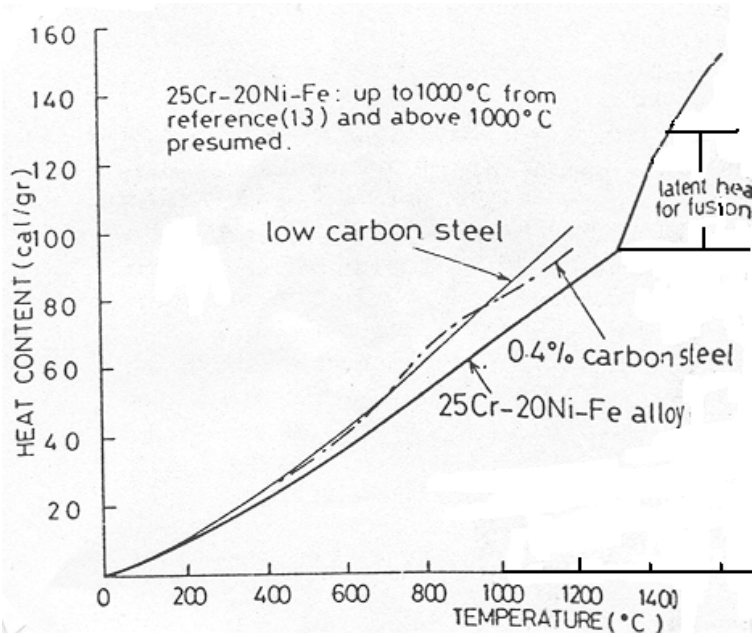

Fig4.3 Heat contents of 25% Cr – 20% Ni –Fe alloy and carbon steels [Ebisu, 1977]

For 0.4% carbon steel –

0 to 125 ^{0}C: $H = 0.8 * 10^{-4} T^2 + 0.10 T$

125 to 550 ^{0}C: $H = 0.4705 * 10^{-4} T^2 + 0.1082 T – 0.51$

550 to 675 ^{0}C: $H = 1.6 * 10^{-4} T^2 - 0.016 T + 33.6326$

For 25 Cr-20 Ni steel –

0 to 1000 ^{0}C: $H = 0.265 * 10^{-4} T^2 + 0.1130 T$

1000 to 1300 ^{0}C: $H = 0.15 * 10^{-4} T^2 + 0.1082 T – 11.50$

1300 to 1400 ^{0}C: $H = 0.6 * T – 589.35$

1400 to 1600 ^{0}C: $H = 0.3 T –169.35$

Similarly we can find *H-T* relationship for other metals also, if we know the variation of specific heat with temperature for that metal.

Equations for *Φ-T* relationship –

The equation for ϕ-T can be calculated from Eq. $\phi = \int_{Td}^{T} \frac{k}{k_d} dT$, if we know the variation of thermal conductivity with temperature. Variation of thermal conductivity with temperature for some metals is shown in fig 4.4.

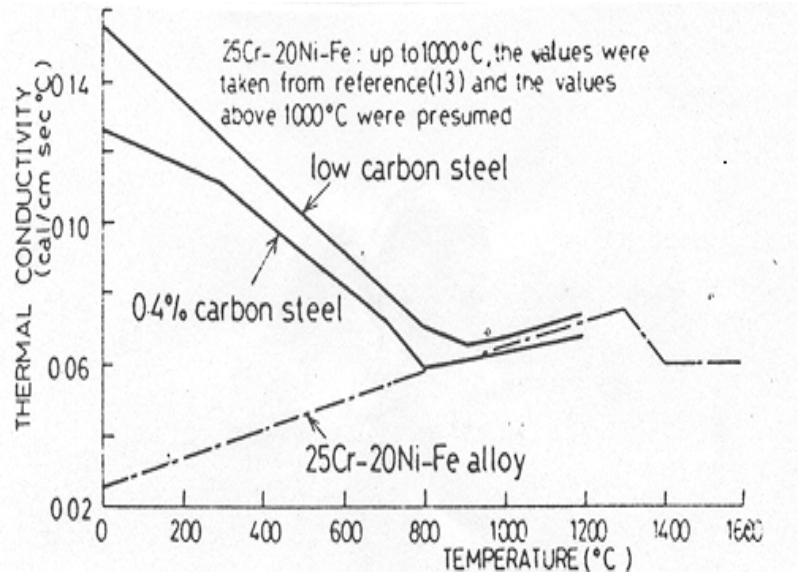

Fig 4.4 Thermal conductivities of 25% Cr – 20% Ni-Fe alloy and carbon steels [Ebisu, 1977]

Thus, for low carbon steel,

0 to 800 ^{0}C: $\phi = -0.342 * 10^{-3} T^2 + T$

800 to 900 ^{0}C: $\phi = -0.161 * 10^{-3} T^2 + 0.709 T + 115.93$

(k_d = 0.155 cal/ cm sec ^{0}c at 0 ^{0}C)

For 0.4% carbon steel,

0 to 300 ^{0}C: $\phi = -0.23 * 10^{-3} T^2 + T$

300 to 700 ^{0}C: $\phi = -0.23 * 10^{-3} T^2 + 1.0785 T - 13.67$

(k_d = 0.1260 cal/ cm sec ^{0}c at 0 ^{0}C)

For 25 Cr-20 Ni steel,

0 to 800 ^{0}C: $\phi = 0.825 * 10^{-3} T^2 + T$

800 to 1300 ^{0}C: $\phi = 0.48 * 10^{-3} T^2 + 1.55 T - 219.0$

(k_d = 0.025 cal/ cm sec ^{0}c at 0 ^{0}C)

Similarly we can find the relationship for Φ-T for other metals also, if we know the relationship between thermal conductivity and temperature.

4.1.5 Solution Steps

1. The user is required to enter the input data, which includes thermal properties of mold and casting materials, dimensions of casting and mold, pouring temperature, and mold preheat temperature.
2. Initialize the temperature in casting and mold region ($T_c = T_p$, $T_m = T_M$), and calculate the initial temperature at casting/coating layer interface by appropriated condition explained in section 3.3.
3. To take into account the variation of thermal conductivity and specific heat with temperature calculate the value for ϕ and H at every node in casting and mold region by the appropriate ϕ-T relation and H-T relation for the initial temperature.
4. Now find the value of H for next time step from the basic equation (3.2).
5. Back substitute the value of H in H-T relations, and find out the value of temperature at new time.
6. Find the values of ϕ at every node by ϕ-T relationship for new time and, for boundary nodes, value of ϕ is found out by imposing boundary conditions.
7. Now repeat step 3-5 till specified time is reached at which we want to know the temperature distribution.

The fig 4.5 shows the flow chart of the program.

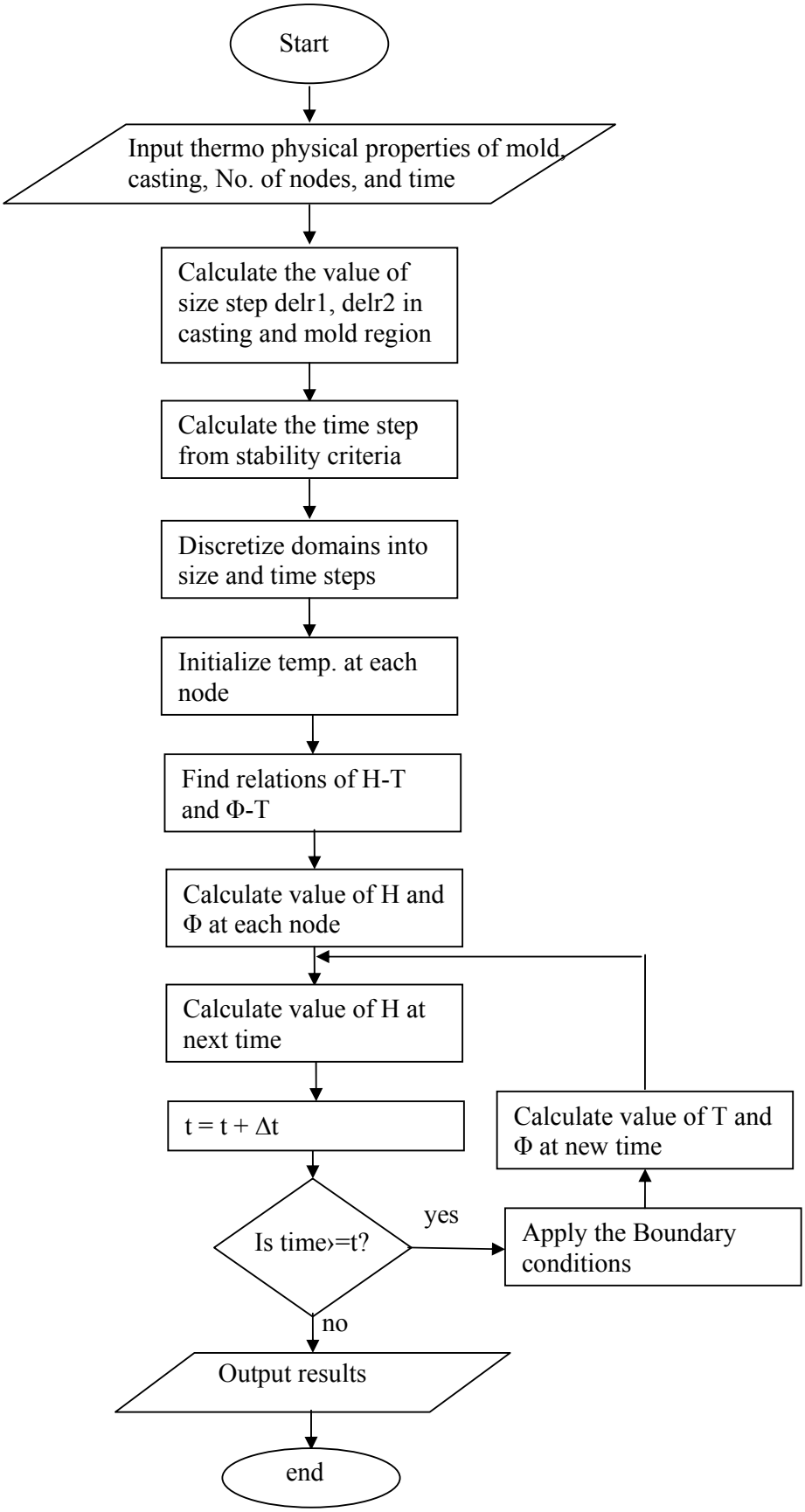

Fig4.5 Flow chart of enthalpy formulation method

4.2 Variable Domain Method

The modeled equations in terms of dimensionless variables in previous chapter have been solved numerically by using simple implicit finite difference technique. For this the "r-t" domain is subdivided into small intervals of constant Δr in space and Δt in time as shown in fig. 4.6. The variable time step approach is used to solve the problem. This approach requires that at each time level t_n the time step Δt_n is so chosen that the interface moves exactly a distance Δr during the time interval Δt, hence always stays on the node. Therefore, the problem is mainly concerned with the determination of the time step $\Delta t = t_{n+1}-t_n$ such that in the time interval from t_n to t_{n+1}, the interface moves from the position $n\Delta r$ to the next position $(n+1)\,\Delta r$.

4.2.1 Finite difference approximation

The differential equation and boundary conditions for both the mold region and casting region can be discretized by using implicit method with the central difference scheme. The thickness of mold region is subdivided into n equal grids, but for casting region the total casting thickness is subdivided into n equal grids. The number of grids in the solid and liquid composite regions varies with time. It means that for the solid composite region the number of grids (n_i) goes on increasing as the solidification proceeds, and for the liquid composite region the number of grids ($n- n_i$) decreases, but their sum always remains same as n.

The differential equations and boundary conditions for both the mold and the casting regions can be discretized by using implicit method with the central difference scheme. To approximate the differential equations in finite difference form, a network of mesh size Δr is constructed over a region which is shown in fig 4.6. It is clear from diagram that the interface moves exactly through one size step in every time step. The variable time step scheme is shown in the figure 4.6.

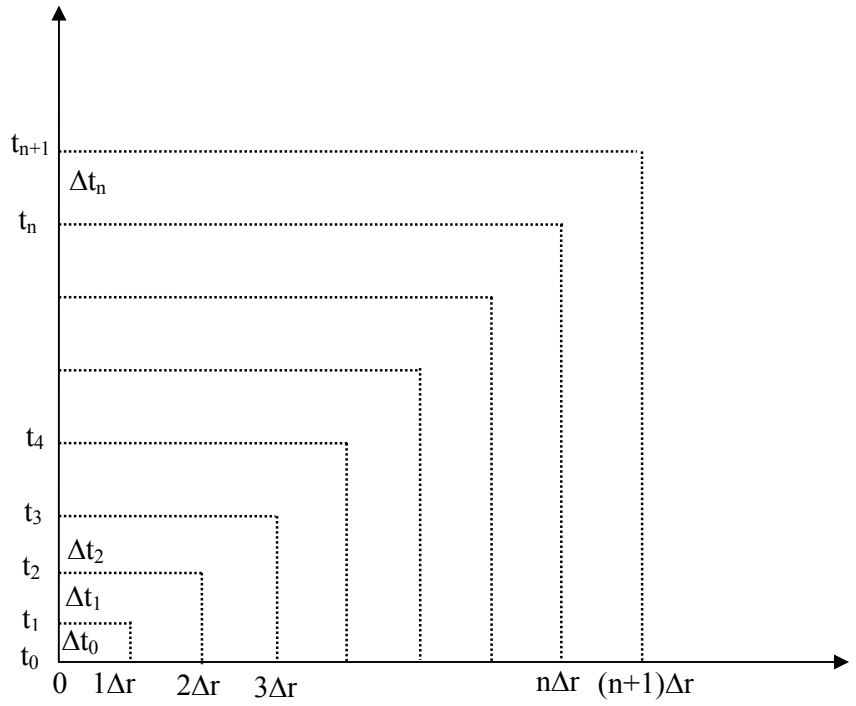

Fig 4.6. Subdivision of "r-t" domain using constant Δr, and variable Δt

Steel Mold Region

Equation (3.1) for the steel mold region is discretized as

$$\frac{T_{m_i}^{p+1} - T_{m_i}^{p}}{\Delta t} = \alpha_m \left[\frac{T_{m_{i-1}}^{p+1} - 2T_{m_i}^{p+1} + T_{m_{i+1}}^{p+1}}{\left(\Delta r_m\right)^2} + \frac{1}{R_{im} + i\Delta r_m} \frac{T_{m_{i+1}}^{p+1} - T_{m_{i-1}}^{p+1}}{2\Delta r_m} \right] \text{..... (4.10)}$$

where

$$\Delta r_m = \frac{R_{om} - R_{im}}{n} \text{..... (4.11)}$$

Equation (4.10) is rearranged in the following form

$$-r_m \left(1 - \frac{0.5}{\frac{R_{im}}{\Delta r_m} + i} \right) T_{m_{i-1}}^{p+1} + \left(1 + 2r_m\right) T_{m_i}^{p+1} - r_m \left(1 + \frac{0.5}{\frac{R_{im}}{\Delta r_m} + i} \right) T_{m_{i+1}}^{p+1} = T_{m_i}^{p} \text{..... (4.12)}$$

where

$$r_m = \frac{\alpha_m \Delta t}{\left(\Delta r_m\right)^2} \quad \text{..... (4.13)}$$

At the outer surface of the steel mold the boundary condition Eq. (3.12) is discretized as

$$-k_m \frac{T_{m_{n+1}}^{p+1} - T_{m_{n-1}}^{p+1}}{2\Delta r_m} = h_2 \left(T_{m_n}^{p+1} - T_a\right) \quad \text{..... (4.14)}$$

The temperature term corresponding to the fictitious node n+1 can be eliminated by combining Eq. (4.12) at node n and Eq. (4.14). This results in equation corresponding to the outer surface of the steel mold, i.e., at the node n, in the following form:

$$-2r_m T_{m_{n-1}}^{p+1} + \left[1 + 2r_m + K_1 r_m \left(1 + \frac{0.5}{\frac{R_{im}}{\Delta r_m} + i}\right)\right] T_{m_n}^{p+1} = K_1 r_m \left(1 + \frac{0.5}{\frac{R_{im}}{\Delta r_m} + i}\right) T_a + T_{m_n}^{p} \quad \text{... (4.15)}$$

where

$$K_1 = \frac{2h_2 \Delta r_m}{k_m} \quad \text{..... (4.16)}$$

Similarly for the inner surface of the steel mold the boundary condition Eq. (3.17) is discretized as

$$-k_m \frac{T_{m_1}^{p+1} - T_{m_{-1}}^{p+1}}{2\Delta r_m} = K . \frac{T_{sc_0,t} - T_{m_0,t}}{d} . \exp(-\beta s(t)) \quad \text{..... (4.17)}$$

By eliminating temperature term corresponding to the fictitious node -1 through Eq. (4.15) at node 0 and the boundary condition Eq. (4.17), the equation at the inner surface of the steel mold is obtained as:

$$-K_2 r_m \left(1 - \frac{0.5}{\frac{R_{im}}{\Delta r_m} + i}\right) T_{sc_0}^{p+1} + \left[1 + 2r_m + K_2 r_m \left(1 - \frac{0.5}{\frac{R_{im}}{\Delta r_m} + i}\right)\right] T_{m_0}^{p+1} - 2r_m T_{m_1}^{p+1} = T_{m_0}^{p} \quad \text{... (4.18)}$$

where

$$K_2 = \frac{2K\Delta r_m}{d . k_m} \cdot \exp(-\beta s(t)) \quad \text{..... (4.19)}$$

Solid Region

Equation (3.24) for the solid region can be discretized as

$$\frac{T_{sc_i}^{p+1}-T_{sc_i}^{p}}{\Delta t}=\frac{\alpha_{sc}}{\left(s(t)\right)^2}\frac{T_{sc_{i-1}}^{p+1}-2T_{sc_i}^{p+1}+T_{sc_{i+1}}^{p+1}}{\left(\Delta\xi\right)^2}+\frac{1}{s(t)}\left[i\Delta\xi\frac{\Delta s(t)}{\Delta t}-\frac{\alpha_{sc_i}}{R_{oc}-i\Delta\xi s(t)}\right]\frac{T_{sc_{i+1}}^{p+1}-T_{sc_{i-1}}^{p+1}}{2\Delta\xi} \quad \text{…. (4.20)}$$

where

$$\Delta\xi=\frac{1}{n_i} \quad \text{…….. (4.21)}$$

Equation (4.20) is rearranged as

$$-r_{sc_i}\left(1-0.5A\right)T_{sc_{i-1}}^{p+1}+\left(1+2r_{sc_i}\right)T_{sc_i}^{p+1}-r_{sc_i}\left(1+0.5A\right)T_{sc_{i+1}}^{p+1}=T_{sc_i}^{p} \quad \text{…… (4.22)}$$

where

$$r_{sc_i}=\frac{\alpha_{sc_i}\Delta t}{\left(s(t)\Delta\xi\right)^2} \quad \text{…….. (4.23)}$$

$$A=\frac{i\left(\Delta\xi\right)^2 s(t)}{\alpha_{sc_i}}\frac{\Delta s(t)}{\Delta t}-\frac{1}{\frac{R_{oc}}{\Delta\xi s(t)}-i} \quad \text{…….. (4.24)}$$

At outer surface of the casting the boundary condition Eq. (3.17) is discretized as

$$\frac{k_{sc_i}}{s(t)}\frac{T_{sc_1}^{p+1}-T_{sc_{-1}}^{p+1}}{2\Delta\xi}=K.\frac{\left(T_{sc_0}^{p+1}-T_{m_o}^{p+1}\right)}{d}.\exp(-\beta s(t)) \quad \text{…… (4.25)}$$

Eliminating the temperature term corresponding to the fictitious node -1 by combining Eq. (4.22) at node 0 and the boundary condition given Eq. (4.25) results in equation which incorporates the outer surface of the casting

$$-K_3 r_{sc_i}\left(1-0.5A\right)T_{m_0}^{p+1}+\left[1+2r_{sc_i}+K_3 r_{sc_i}\left(1-0.5A\right)\right]T_{sc_0}^{p+1}-2r_{sc_i}T_{sc_i}^{p+1}=T_{sc_0}^{p} \quad \text{… (4.26)}$$

where

$$K_3=\frac{2s(t)\Delta\xi}{k_{sc_i}}\cdot\frac{K}{d}\cdot\exp\left(-\beta s(t)\right) \quad \text{…….. (4.27)}$$

Liquid Region

Eq. (3.27) for liquid region is descretized as

$$\frac{T_{lc_i}^{p+1}-T_{lc_i}^{p}}{\Delta t}=\frac{1}{r_i-s(t)}\left[(1-i\Delta\eta)\frac{\Delta s(t)}{\Delta t}-\frac{\alpha_{lc_i}}{\left(R_{oc}-s(t)-i\Delta\eta\left(r_i-s(t)\right)\right)}\right]\frac{T_{lc_{i+1}}^{p+1}-T_{lc_{i-1}}^{p+1}}{2\Delta\eta}+\frac{\alpha_{lc_i}}{\left(r_i-s(t)\right)^2}\frac{T_{lc_{i-1}}^{p+1}-2T_{lc_i}^{p+1}+T_{lc_{i+1}}^{p+1}}{(\Delta\eta)^2} \quad \ldots\ldots\ldots\ldots\ldots\ldots (4.28)$$

where

$$\Delta\eta=\frac{1}{n-n_i} \quad \ldots\ldots\ldots\ldots\ldots\ldots\ldots\ldots\ldots\ldots\ldots\ldots\ldots\ldots\ldots\ldots (4.29)$$

Equation (4.28) can be rearranged as

$$-r_{lc_i}\left(1-0.5B\right)T_{lc_{i-1}}^{p+1}+\left(1+2r_{lc_i}\right)T_{lc_i}^{p+1}-r_{lc_i}\left(1+0.5B\right)T_{lc_{i+1}}^{p+1}=T_{lc_i}^{p} \ldots\ldots\ldots\ldots (4.30)$$

where

$$r_{lc_i}=\frac{\alpha_{lc_i}\Delta t}{\left(\left(r_i-s(t)\right)\Delta\eta\right)^2} \quad \ldots\ldots\ldots\ldots\ldots\ldots\ldots\ldots\ldots\ldots\ldots\ldots\ldots\ldots\ldots\ldots (4.31)$$

$$B=\frac{\left(1-i\Delta\eta\right)\Delta\eta\left(r_i-s(t)\right)}{\alpha_{lc_i}}\frac{\Delta s(t)}{\Delta t}-\frac{1}{\frac{R_{oc}-s(t)}{\Delta\eta\left(r_i-s(t)\right)}-i} \quad \ldots\ldots\ldots\ldots\ldots\ldots\ldots\ldots\ldots\ldots\ldots\ldots\ldots\ldots\ldots\ldots (4.32)$$

At the inner surface of the casting the boundary condition Eq. (3.14) is discretized as

$$\frac{-k_{lc_i}}{r_i-s(t)}\frac{T_{lc_{n+1}}^{p+1}-T_{lc_{n-1}}^{p+1}}{2\Delta\eta}=h_1\left(T_{lc_n}^{p+1}-T_a\right) \ldots\ldots\ldots\ldots\ldots\ldots\ldots\ldots\ldots\ldots\ldots\ldots\ldots\ldots\ldots\ldots (4.33)$$

The temperature term corresponding to the fictitious node n+1 is eliminated by combining Eq. (4.30) at node n and the boundary condition Eq. (4.33), resulting in the equation incorporating the inner surface of the casting as

$$-2r_{lc_i}T_{lc_{n-1}}^{p+1}+\left(1+2r_{lc_i}+K_4r_{lc_i}\left(1+0.5B\right)\right)T_{lc_n}^{p+1}=K_4r_{lc_i}\left(1+0.5B\right)T_a+T_{lc_n}^{p} \ldots (4.34)$$

where

$$K_4=\frac{2h\Delta\eta\left(r_i-s(t)\right)}{k_{lc_i}} \quad \ldots\ldots\ldots\ldots\ldots\ldots\ldots\ldots\ldots\ldots\ldots\ldots\ldots\ldots\ldots\ldots\ldots\ldots (4.35)$$

At Solid-Liquid Interface

Equation (3.28), representing the condition of continuity of temperature at the interface, are written as

$$T_{lc_{n_i}}^{p+1} = T_{sc_{n_i}}^{p+1} = T_f \quad \text{..... (4.36)}$$

Equation (3.30) representing the energy balance at the solid-liquid interface is discretized as

$$\frac{k_{sc_{n_i}}}{s(t)} \frac{T_{sc_{n_i}}^{p+1} - T_{sc_{n_i-1}}^{p+1}}{\Delta\xi} = \frac{k_{lc_{n_i}}}{r_i - s(t)} \frac{T_{lc_{n_i+1}}^{p+1} - T_{lc_{n_i}}^{p+1}}{\Delta\eta} + \rho_{sc_{n_i}} \Delta H \frac{\Delta s(t)}{\Delta t} \quad \text{..... (4.37)}$$

Equation (4.37) is rearranged in the form

$$\Delta t = \frac{\rho_{sc_{n_i}} \Delta H \Delta s(t)}{k_{sc_{n_i}}} \left[\frac{1}{\frac{1}{s(t)} \frac{T_f - T_{sc_{n_i-1}}^{p+1}}{\Delta\xi} - \frac{k_{lc_{n_i}}}{k_{sc_{n_i}}} \frac{1}{r_i - s(t)} \frac{T_{lc_{n_i+1}}^{p+1} - T_f}{\Delta\eta}} \right] \quad \text{..... (4.38)}$$

Equations for different regions are solved with boundary conditions using implicit finite difference scheme. The resultant discretized equations are arranged in tridiagonal matrix form and the solution of these equations can be obtained by using Thomas Algorithm (TDMA), which will give temperature distribution in both casting and mold regions for a particular time step Δt_n.

4.2.2 Determination of time steps

During solidification the interface moves from the position nΔr to the position (n+1) Δr within a time interval of $\Delta t_i = t_{i+1} - t_i$ (shown in fig. 4.7), which is not know in a priori.

Using modified variable tiem step (MVTS) method the actual value of Δt_i is obtained by iteration as follows [Gupta, and Kumar, 1981]:

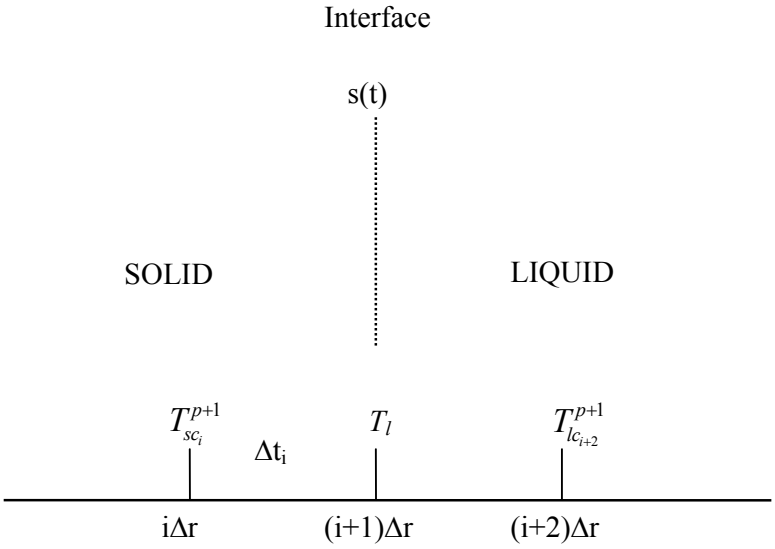

Fig 4.7. Representation of Interface at s(t) =(i+1)Δr

1. An initial guess value for the time step Δt_i chosen as $\Delta t_i = \Delta t_i^{(0)}$.
2. Using $\Delta t_i^{(0)}$, first estimate for the nodal temperatures is obtained by solving the finite difference equations for the mold and casting regions.
3. First estimate for the time step $\Delta t_i^{(1)}$ is obtained by using estimates $[T_{lc_{n_{i+1}}}^{p+1}]$ and $[T_{sc_{n_{i-1}}}^{p+1}]$ in equation (4.38).
4. Using $\Delta t_i^{(1)}$ repeat the steps (2) and (3) to obtain $\Delta t_i^{(2)}$
5. Iteration is carried out until the difference between the two consecutive time steps satisfies as specified convergence criterion.
6. To obtain Δt_{i+1} assume $\Delta t_{i+1}^{(0)i} = \Delta t_i$ and repeat the steps from (2) to (5).
7. Repeat steps from (2) to (6) till the solid-liquid interface reaches the inner surface of the casting.

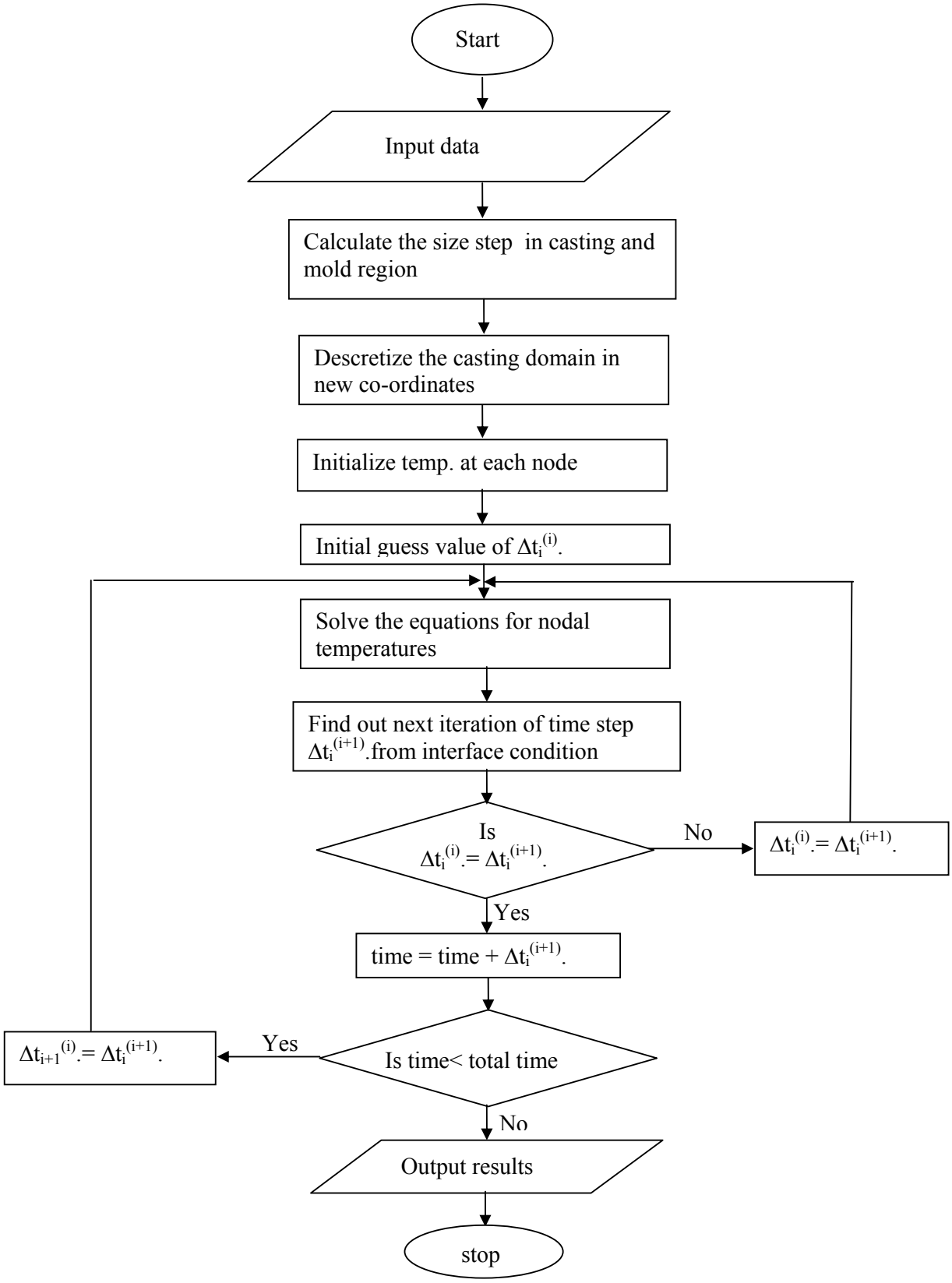

Fig 4.8. Flow chart of Variable domain method

4.3 Calculation of *h* at outer surface of mold

The heat transfer between the casting mold and ambient is treated as a horizontally rotating body in static air. In a real casting condition, *Gr/Re* is less than 0.1 and $Re>5*10^5$; therefore, the natural convection could be neglected, and the heat transfer coefficient is approximated in terms of the following equation of dimensionless correlation [Yang et al, 1994, Kendoush, 1996]:

$$N_u = \frac{R_e P_r \sqrt{C_D/2}}{5P_r + 5\ln(3P_r+1)} + \sqrt{C_D/2} - 12 \quad \text{..... (4.39)}$$

$$Nu = 0.6366\left(\mathrm{Re}\,\mathrm{Pr}\right)^{0.5} \quad \text{..... (4.40)}$$

Where

$R_e = \omega D^2/\nu$, $N_u = hD/k$ and $P_r = \nu/\alpha$

h is the average heat transfer coefficient

ω represents the angular rotation velocity of the mold

C_D is the resistance coefficient of mold surface

υ and α are viscosity and thermal diffusivity of the air, respectively.

The temperature of evaluation properties is $T_i = (T_\omega + T_a)/2$ and T_ω and T_a are temperature on the outer surface of casting mold and ambient temperature.

The centrifugal force acting on the molten metal is given by

$$F_c = m\omega^2 r \quad \text{..... (4.41)}$$

Where:

m = mass of metal being poured;

ω = rotation speed of mold;

r = radius of rotation

Since the weight and radius of rotation are determined by casting dimensions, spinning speed is the only variable for the action of centrifugal force.

Because gravity acts with a constant magnitude and in vertical direction, any change in the combined action of these two forces must come through changing one of two things: either the angle of the spinning axis to the horizontal or the speed of the spin. The position of the spinning axis in casting machines is usually chosen to fit with the

type of casting being made. If the axis angle is kept constant during the casting operation, the spinning speed can be used to control the effects given to metal by the combined forces. The following graph shows the speed curves for centrifugal casting to choose the optimum rotation speed of mold.

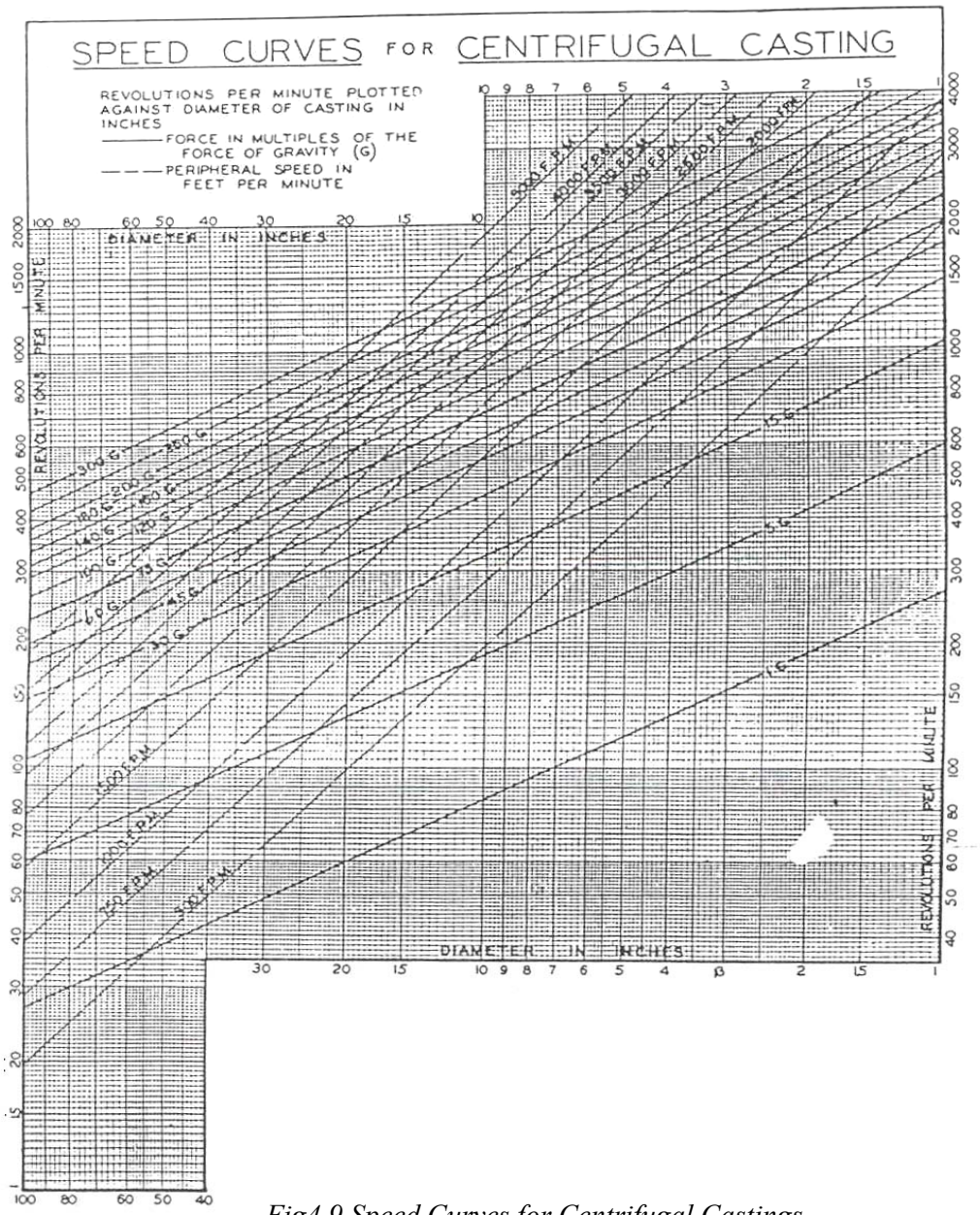

Fig4.9 Speed Curves for Centrifugal Castings

The solution procedure explained in this chapter is implemented in computer program, and results obtained by the computer program are presented in the next chapter.

Chapter 5

Results and Discussion

The computer program has been has developed to solve the equations developed in previous chapters. The solution steps and flow chart for the program are shown in previous chapter. The modeled equations are solved to evaluate solidification time, and temperature distribution within the casting as well as in the mold region for different process parameters. Due to axial symmetry in centrifugal castings the problem reduced to two dimensional, but for simplicity the present work analyses only one dimensional situation in the radial direction. It can be mentioned here that the results calculated using developed software program in this work are compared with the results available in the literature for similar conditions. The results are available for similar situation in reference [Ebisu, 1977].

The model has been implemented by using following thermo physical properties (for casting and mold material), and design and operating parameters. 25% Cr-20% Ni steel is chosen as molten metal and 0.4% Carbon steel as mold material to validate the developed model with results available in literature. Various design and operating parameters, like geometric constants for the casting and the mold, the heat transfer co-efficient at different regions of casting and the mold, and initial temperatures of mold and metal used in simulation are tabulated in Table 5.2. The cooling conditions at the inner surface of the casting and at the outer surface of the steel mold are defined in terms of heat transfer coefficients h_1, h_2 respectively, and the heat transfer due to the air gap at the metal-mold interface is varied by the solidified thickness of casting. The results of simulation are presented in the following sections.

Casting material: 25% Cr-20% Ni steel

Mold material: 0.4% Carbon steel

$\epsilon_M = 0.4$, the value at approximately 300 ^{0}C for the OD of mold.

Coating layer: Silica flour, diatomaceous earth and binder diluted with water

Table 5.1: Thermo physical properties of casting, mold material, and coating layer

Thermo physical Properties	25% Cr-20% Ni steel	0.4% Carbon steel	Coating layer
K_d (cal/cm sec ^{0}C) at 0 ^{0}C	0.025	0.1260	2* 10^{-2}
ρ (gr/cm^3)	7.3	7.8	5.7
C (cal/gm ^{0}C)	0.118	0.1	0.08
T_S(^{0}C)	1300	_	_
T_L(^{0}C)	1400	_	_
T_f(^{0}C)	1300	_	_
ΔH (cal/gr)	60	_	_

Table 5.2: Design and operating parameters used in simulation

Outer dia. of steel mold, D_3 (cm)	31.0
Outer dia of casting, D_2 (cm)	13.0
Inner dia. of casting, D_1 (cm)	9.0
Damping coefficient between the mold-metal interface, β	0.83
Heat transfer coefficient at outer surface of steel mold (h_2) and at inner surface of casting (h_1) (cal/cm^2 sec ^{0}C)	0.0002
Initial pouring temperature of liquid metal, T_p (^{0}C)	1500
Initial mold temperature, T_M (^{0}C)	350
Ambient temperature, T_a (^{0}C)	25
Emissivity at outer surface of mold ϵ_M	0.4

5.1 Temperature profiles in casting and mold region

The temperature profiles in the casting as well as mold regions have been calculated solving the energy balance equations along with the appropriate boundary conditions; by both fixed domain as well as variable domain method for the different pouring temperature and mold preheat temperature. Following graphs show the temperature profiles in the casting and mold regions at different times with different initial conditions for both the methods. As shown in graph the temperature of molten metal falls below the solidus temperature between times 60-100 seconds, the complete metal solidifies at this time. These solidification times are in reasonable limit of 1-2 minutes, in foundry practice [Ebisu, 1977].

5.1.1 Fixed Domain Method (Enthalpy Formulation)

The following graphs for the temperature profile in casting and mold regions have been obtained by using the physical properties and operating condition mentioned above. The temperature profiles in casting and mold region has been analyzed for different pouring temperature, and molds preheat temperature. The temperature profiles have been obtained with pouring temperatures (150-200 ^{0}C above solidus temperature) to analyze the results with mold preheat temperature 350 ^{0}C. In order to save the mold from the thermal shock at the starting of solidification, the mold preheat temperature of 250-375 ^{0}C have been used. The following graphs show the temperature profile in casting and mold regions at different time for the some set of pouring temperature and mold preheat temperature. It is clear from the graphs that due to the formation of air-gap between casting and mold after some time, as solidification progresses towards inner bore, local heating of inner bore of mold takes place (due to reduction in heat transfer between casting and mold interface). It is evident from the following graphs that the solidification commences from the outer surface of the casting, which is in contact with mold inner surface, and grows towards inner surface of casting. There is some chance of cooling of inner surface of casting below solidus temperature, until solidification front reaches to inner bore, because of heat loss by convection at inner bore of casting. The chances of this to happen are less because the heat transfer coefficient at inner bore is very less.

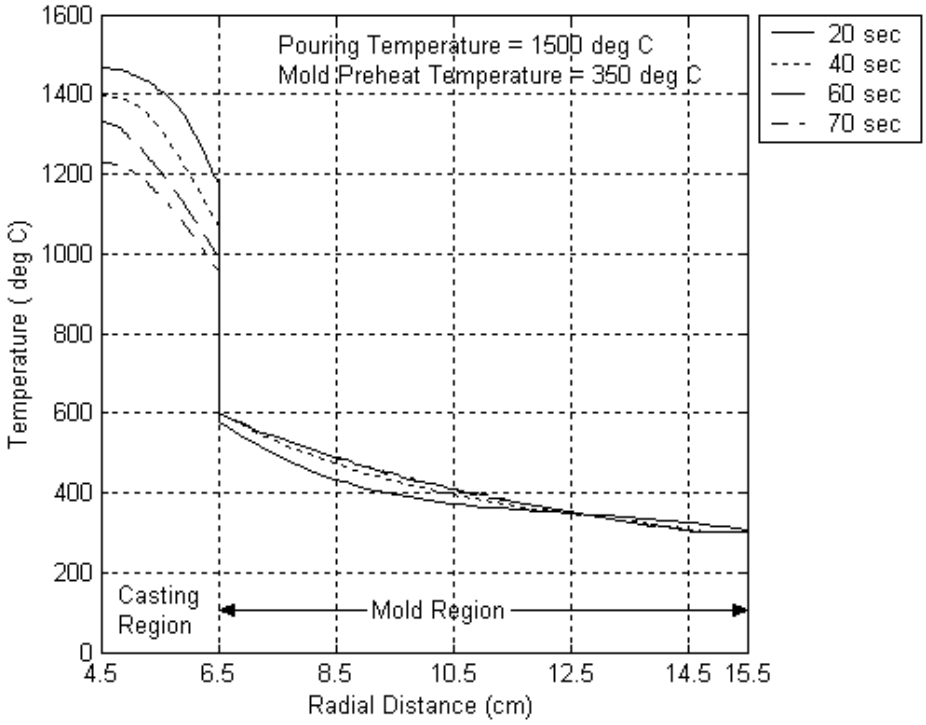

Fig 5.1 Temperature profile in casting and mold region for T_p =1500 ^{0}C

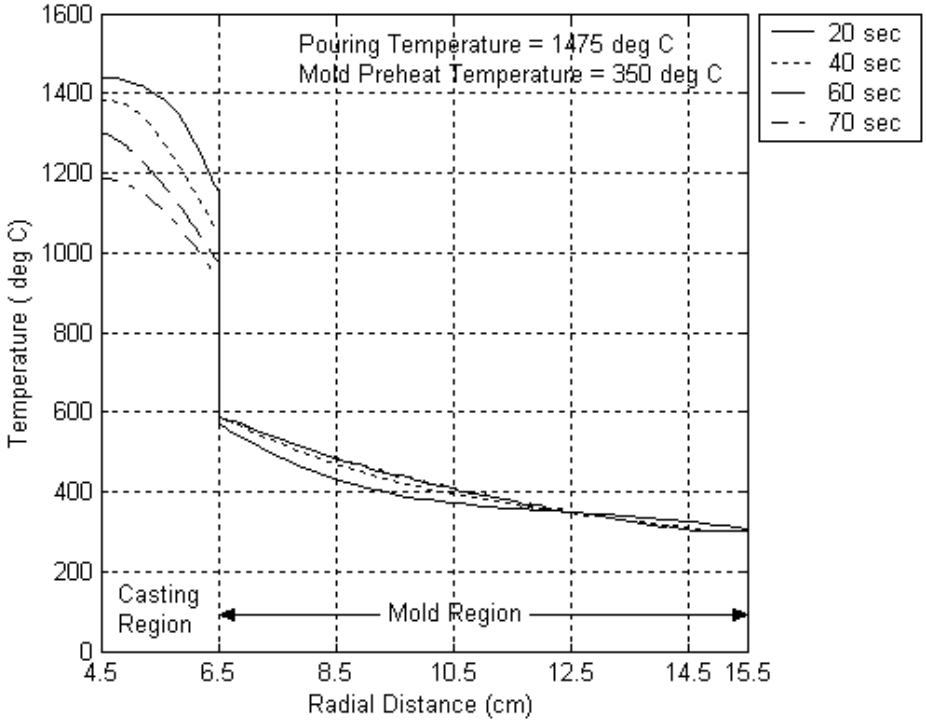

Fig 5.2 Temperature profile in casting and mold region for T_p =1475 ^{0}C

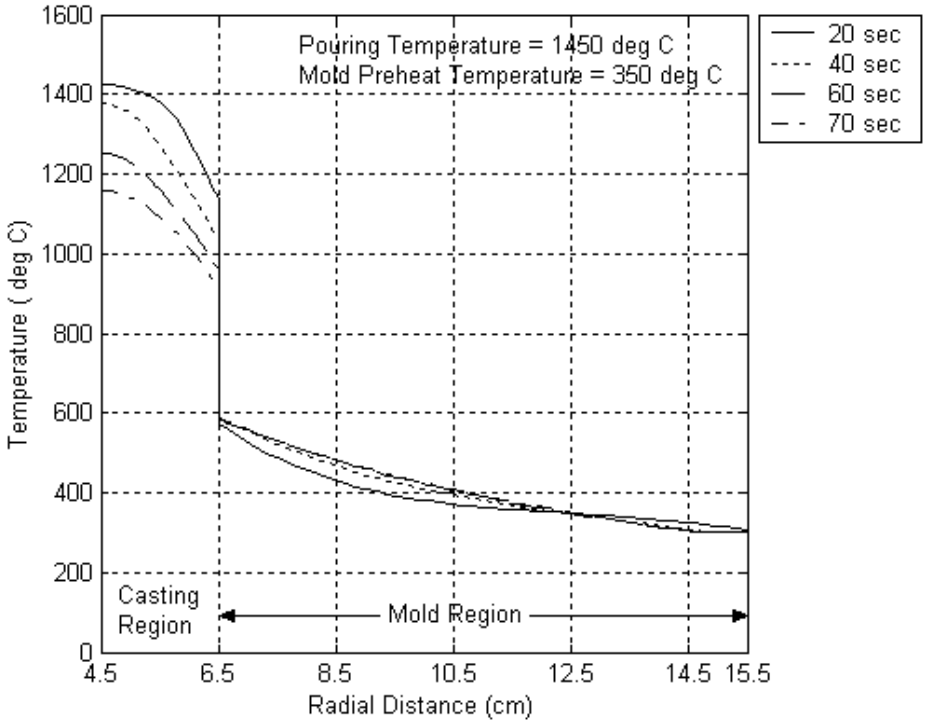

Fig 5.3 Temperature profile in casting and mold region for T_p =1450 ^{0}C

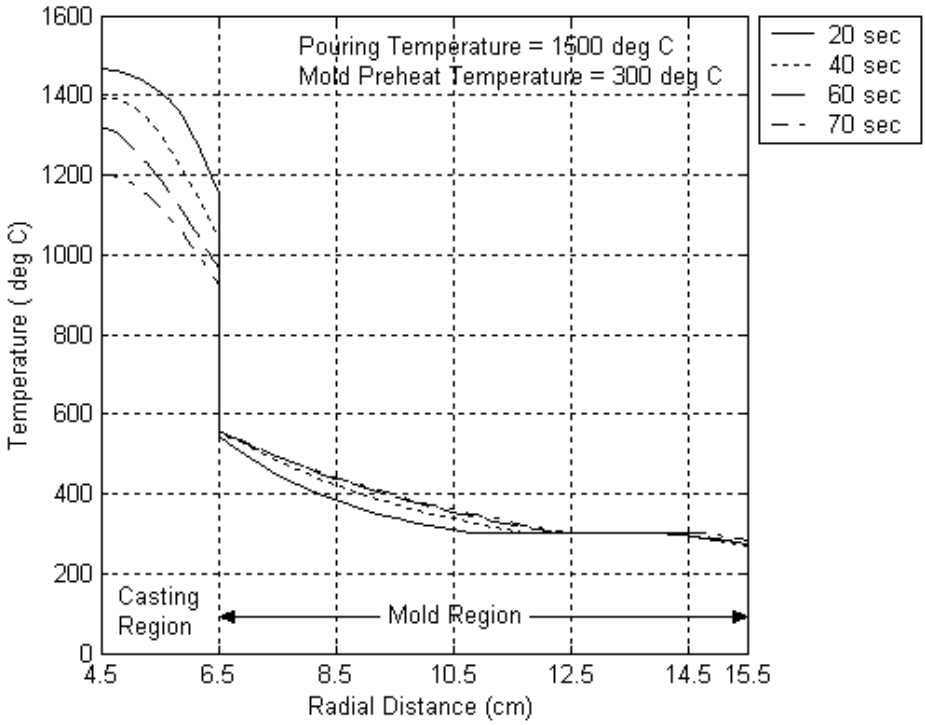

Fig 5.4 Temperature profile in casting and mold region for T_M =300 ^{0}C

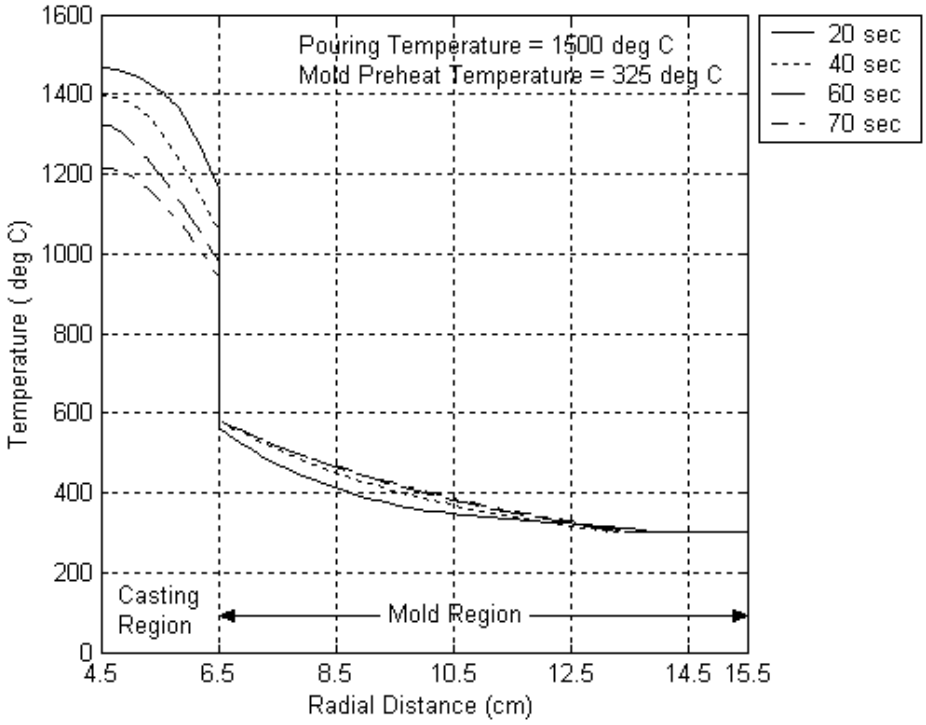

Fig 5.5 Temperature profile in casting and mold region for T_M =325 ^{0}C

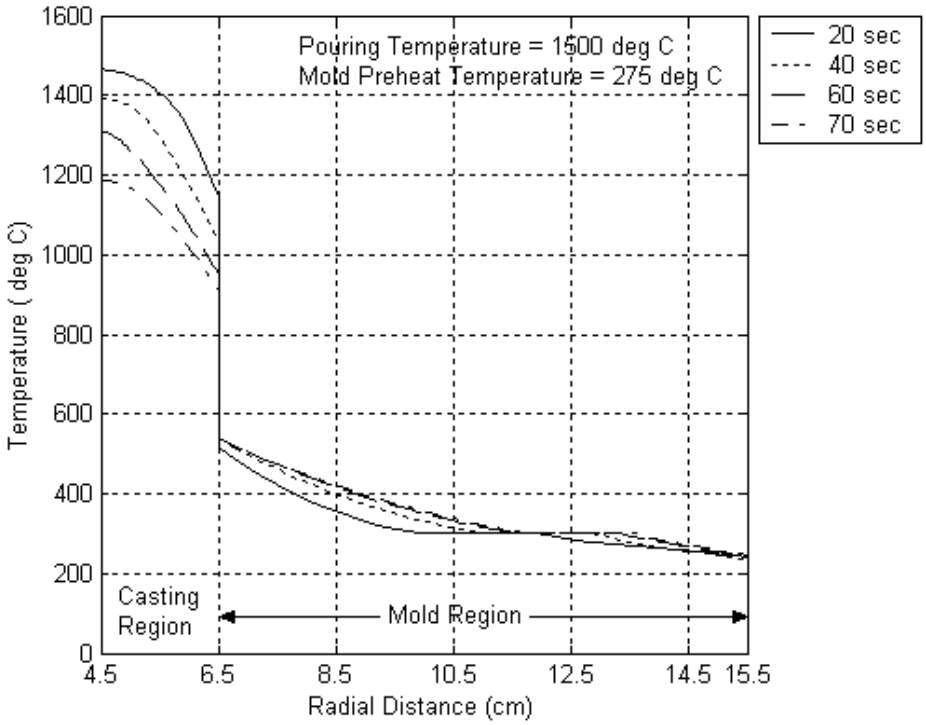

Fig 5.6 Temperature profile in casting and mold region for T_M =275 ^{0}C

5.1.2 Variable Domain Method

The modeled equations for variable domain method have been solved with appropriate boundary conditions to find the temperature profile in casting and mold region. The variable time step method is used to find out the location of interface explicitly at particular time in radial direction. The temperature profile obtained by this method is similar to that Fixed domain method, but solidification time is slightly higher than that obtained by the Fixed domain method. The following graphs show the variation of temperature at different times in mold and casting regions. The characteristics of these graphs are similar to that obtained by the Fixed domain method. To analyze the effect of pouring temperature and mold preheat temperature the different set of pouring and mold preheat temperature is used to plot the graphs.

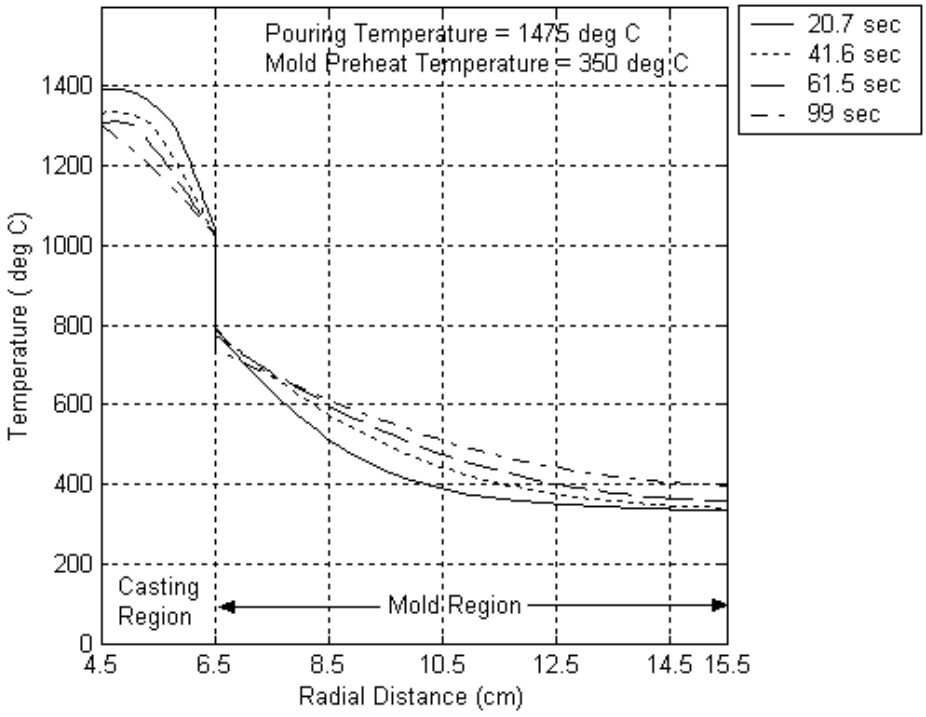

Fig 5.7 Temperature profile in casting and mold region for T_p =1475 ^0C

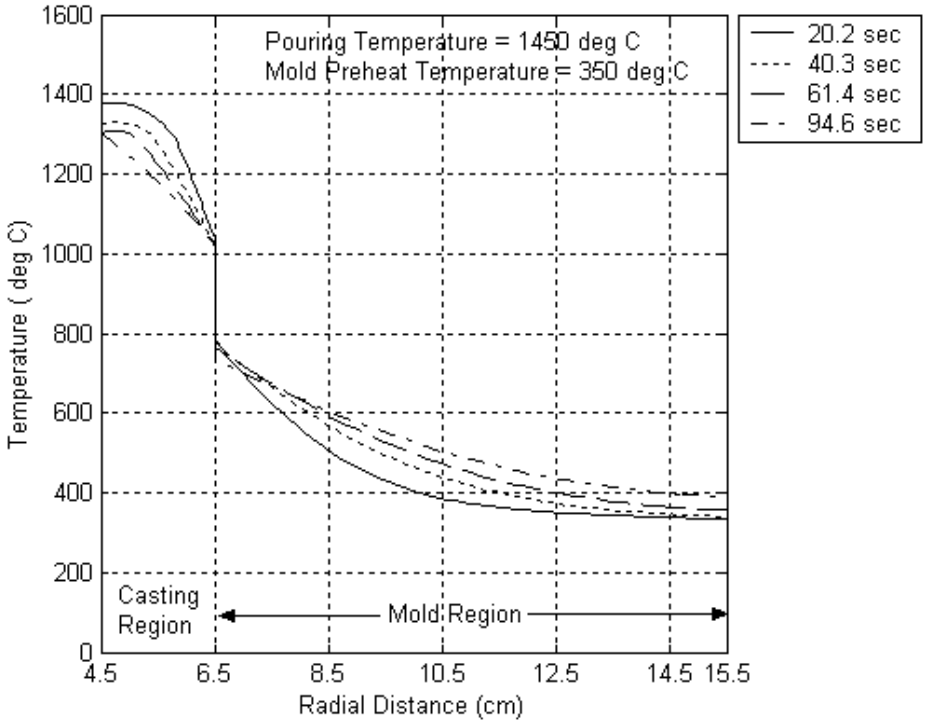

Fig 5.8 Temperature profile in casting and mold region for T_p =1450 ^{0}C

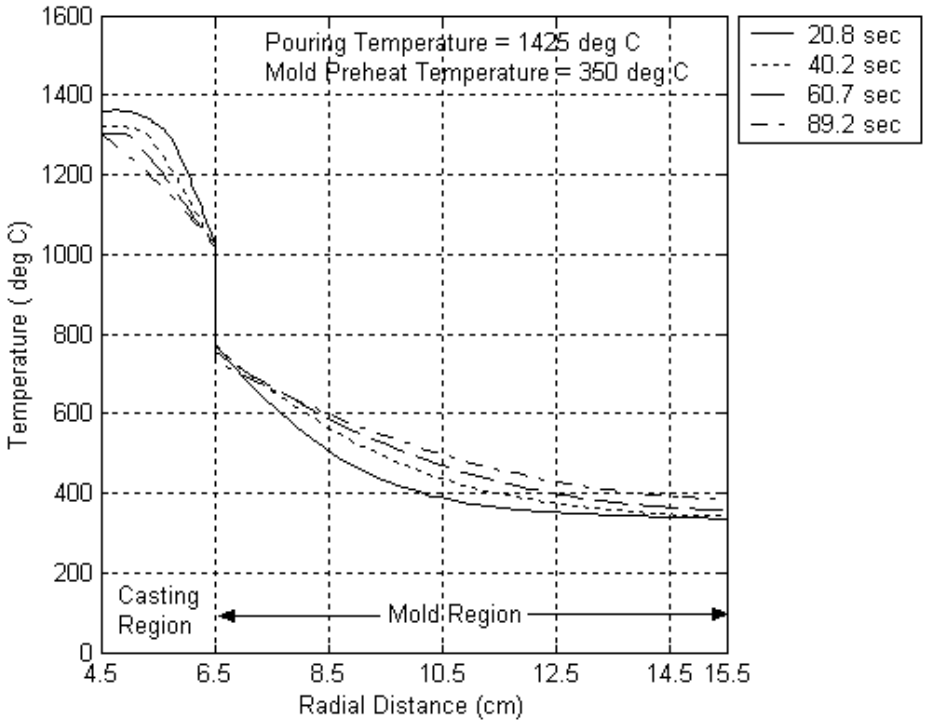

Fig 5.9 Temperature profile in casting and mold region for T_p =1425 ^{0}C

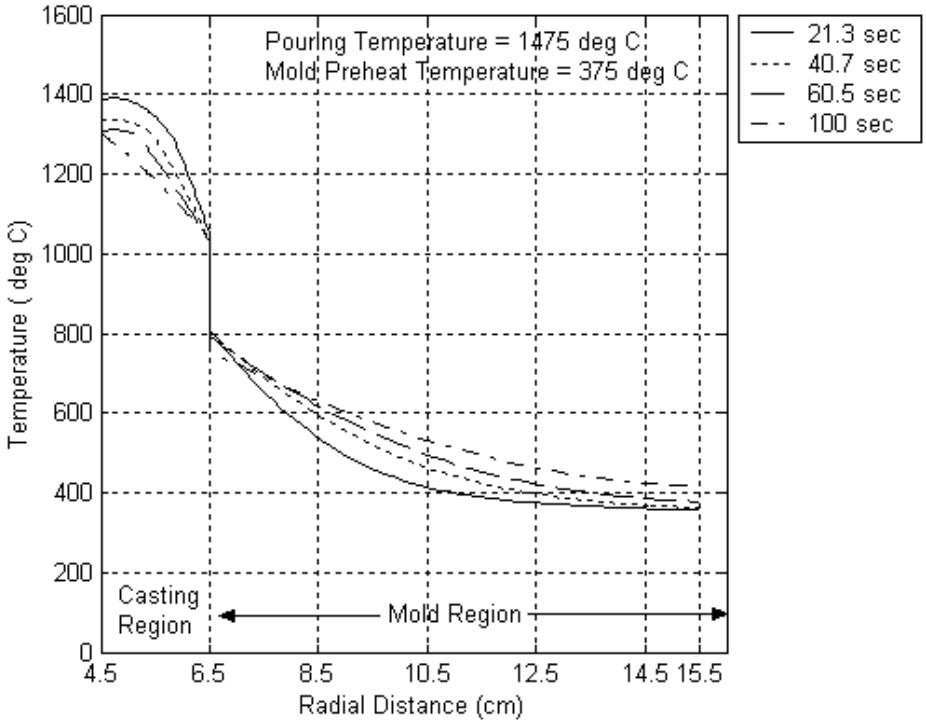

Fig 5.10 Temperature profile in casting and mold region for T_M =375 ^{0}C

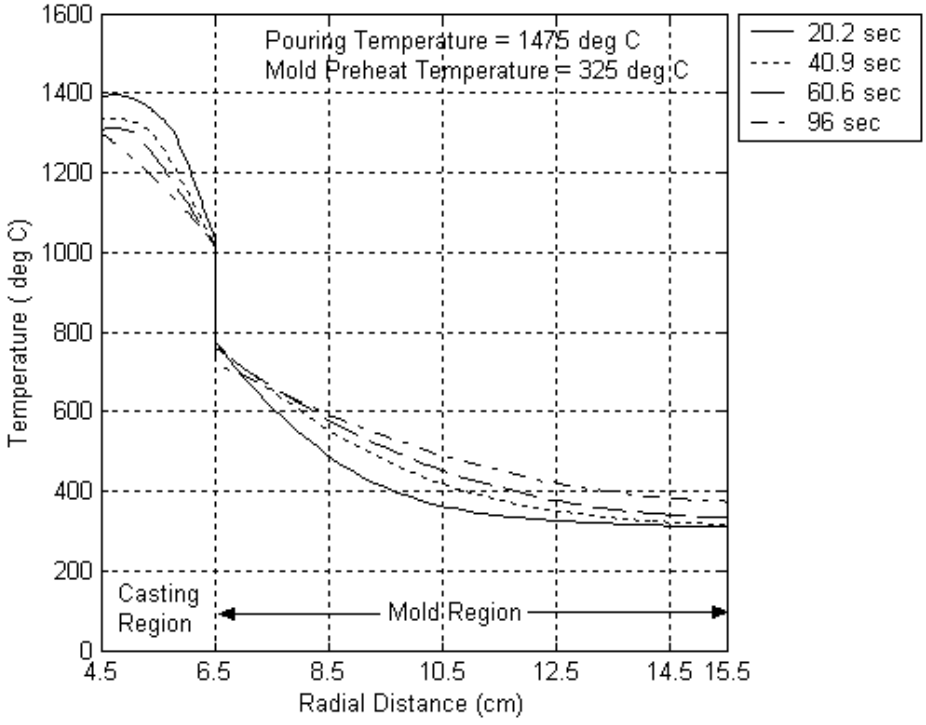

Fig 5.11 Temperature profile in casting and mold region for T_M =325 ^{0}C

5.2 Solidification Time Calculation

For various sets of operating conditions, the time required for complete solidification of the casting has been calculated. Typical results of these calculations are presented in the form of (i) solidified thickness of the shell, and (ii) total solidification time, in the following figs. The main parameters which have effect on solidification rate are the pouring temperature, the mold preheat temperature, and the insulation of coating layer at metal-mold interface, and formation of air gap between metal and mold.

5.2.1 Effect of Initial Pouring Temperature

Following figures shows the development of the solid shell thickness as a function of solidification time for three different initial pouring temperatures. The time for complete solidification of the casting is the time when the shell thickness becomes 2 cm (the casting thickness). It is evident that the time for complete solidification increases with increased pouring temperature of molten metal. This is due to fact that as T_p increases total heat content increases and more time is required to withdraw this excess heat through mold wall. Following figures shows the variation of solidification time as a function of initial pouring temperature for given mold preheat temperature.

5.2.2 Effect of Mold Preheat Temperature

Following figures shows the plot of solidified shell thickness as a function of solidification time for four different initial mold temperatures. From this figures, it is evident that the time required for complete solidification of the casting increases with increasing initial mold temperature. As the initial mold temperature increases, the temperature gradient between the solid region and mold decreases, this in turn reduces the heat transfer rate. This results in longer time for complete solidification of the casting. Thus mold preheat temperature also has significant influence on the solidification time and solidification behavior of casting. The fig 5.12 shows the effect of mold preheat temperature on the solidification time.

Fixed domain method:

The following graphs show the variation of solidification time as function of pouring temperature and mold preheat temperature obtained by fixed domain method.

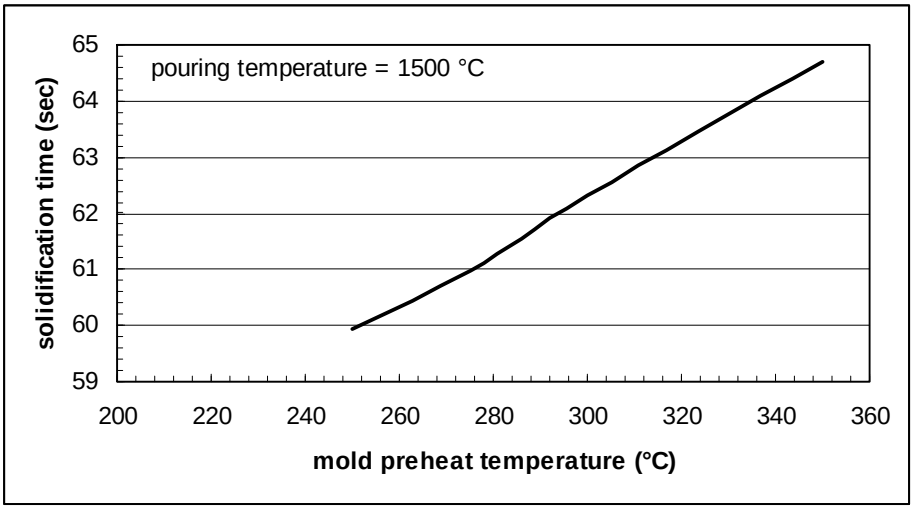

Fig 5.12 Solidification time as function of mold preheat temperature

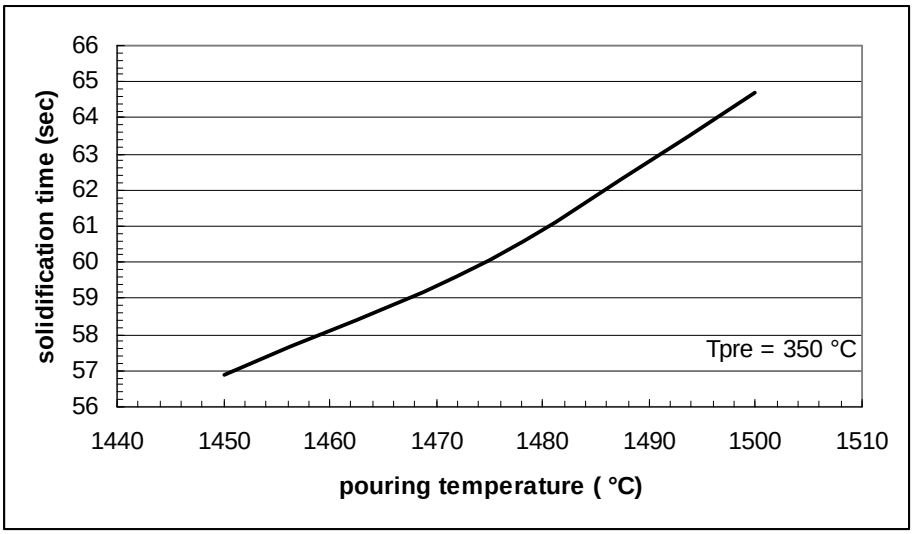

Fig 5.13 Solidification time as function of pouring temperature

Variable Domain Method

By the Variable Domain method, it is possible to track the solid-liquid interface in the radial direction by using modified variable time step method, in which solidification front moves from one grid point to next grid point in every time step. The development of solidified layer is represented as the function of pouring time in following figures for different pouring temperatures and mold preheat temperatures. It is clear from the graphs that the initial heat transfer between casting and mold region is high due to higher thermal gradient between casting and mold interface. Due to the formation of air-gap between casting and mold region, the heat transfer between casting and mold decreases as the solidification commences. Therefore solidification front takes more time to move from one grid point to another after air-gap formation as the solidification progresses. The total solidification time obtained by this method is more than that obtained by previous method, but it is still within the limit of foundry experiences of 1-2 minutes.

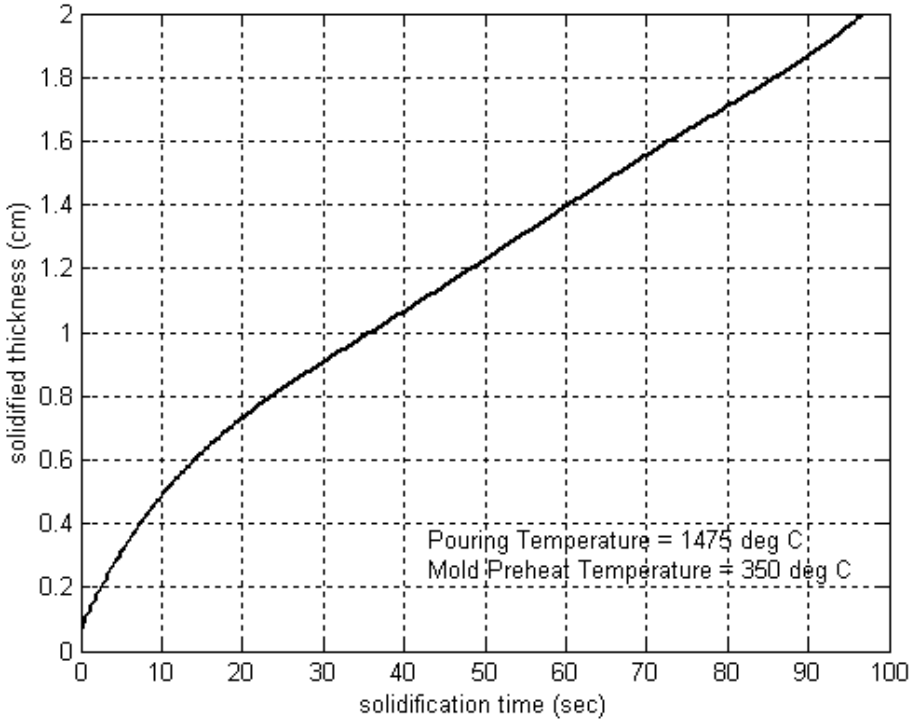

Fig 5.14 Development of solidified thickness as function of solidification time for T_p = 1475 ^0C

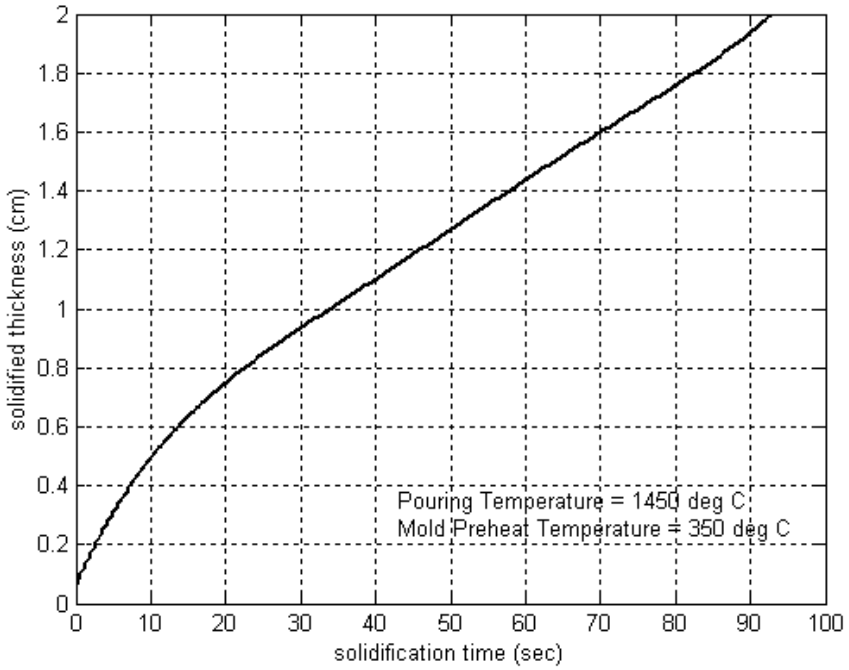

Fig 5.15 Development of solidified thickness as function of solidification time for $T_p = 1450\ ^0C$

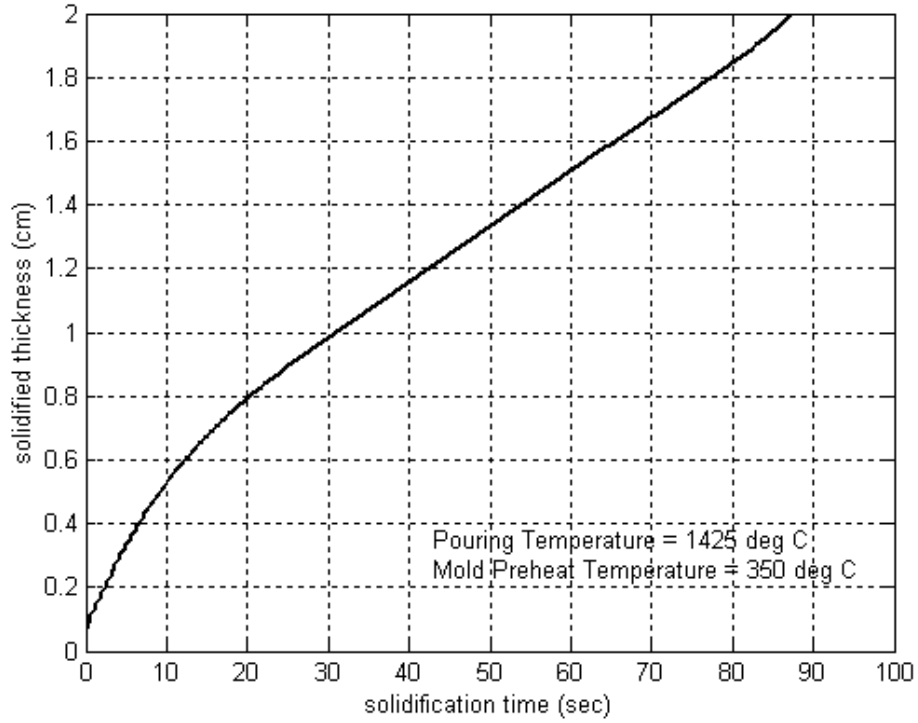

Fig 5.16 Development of solidified thickness as function of solidification time for $T_p = 1425\ ^0C$

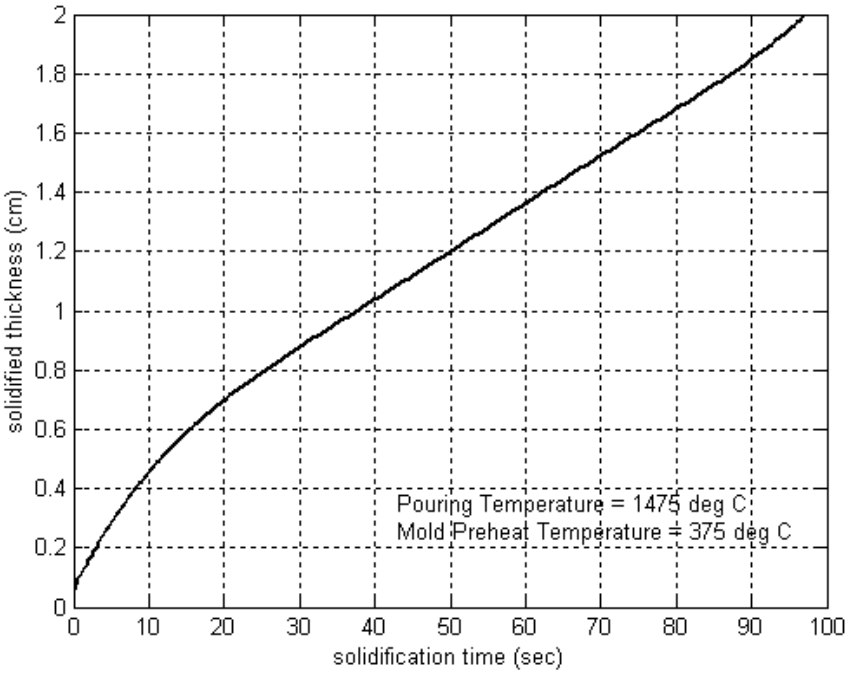

Fig 5.17 Development of solidified thickness as function of solidification time for $T_M = 375\ ^0C$

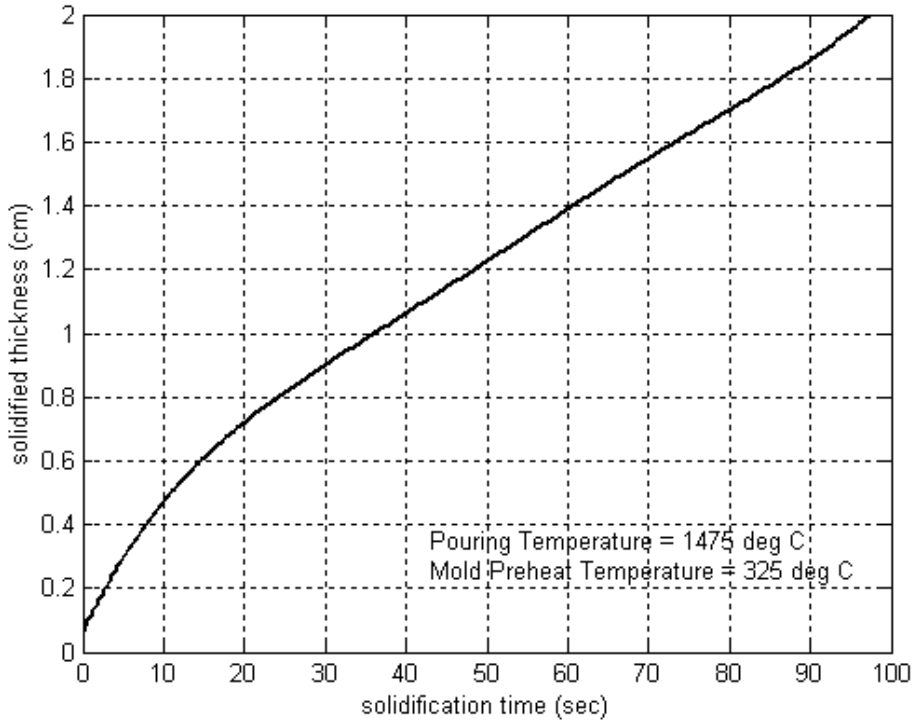

Fig 5.18 Development of solidified thickness as function of solidification time for $T_M = 325\ ^0C$

5.3 Comparison with Results Available in Literature

The following graph shows the result (temperature profile in casting and mold region and total solidification time) obtained by Ebisu [Ebisu, 1977], for similar thermo-physical properties of casting and mold materials, and operating conditions, which have been used in the simulation. The temperature profiles and solidification times obtained by simulation, for different operating conditions have been shown above. It is clear from graphs drawn above and the following graph, that the trend of temperature profiles obtained by both Fixed domain method and Variable domain method is similar to those obtained by Ebisu, with some percent of error. It is evident form graphs for temperature profiles that solidification starts from the molten metal in contact with the inner mold wall and proceeds right across the inner section until last solidifying metal freezes at inner bore, therefore the chances of shrinkage cavity is more at inner bore as compare to other region of solidifying metal.

The major reason for error is the phenomenon happening at the mold-metal interface during solidification of metal. It is very difficult to set the boundary condition at the metal-mold interface since as the solidification proceeds towards inner bore, liquid metal gets contract after solidification and mold material expands due to heating, this results in the formation of air-gap between solidified metal and mold. Due to this phenomenon heat transfer rate decrease as the solidification proceeds, this decrease in the heat transfer rate has been incorporated in model by considering the decrease in the heat conduction through solid-mold interface as the function of solidified thickness. The second reason is the application of variation of thermal properties with the temperature, since the complete data for the variation of these properties with temperature is not available in the literature.

The total solidification time obtained by the both methods is within the reasonable range of 1-2 minutes as mentioned in the paper [Ebisu, 1977]. The total solidification time obtained by Fixed domain method is coming between 60-70 seconds, while by Variable domain method it is coming between 90-100 seconds.

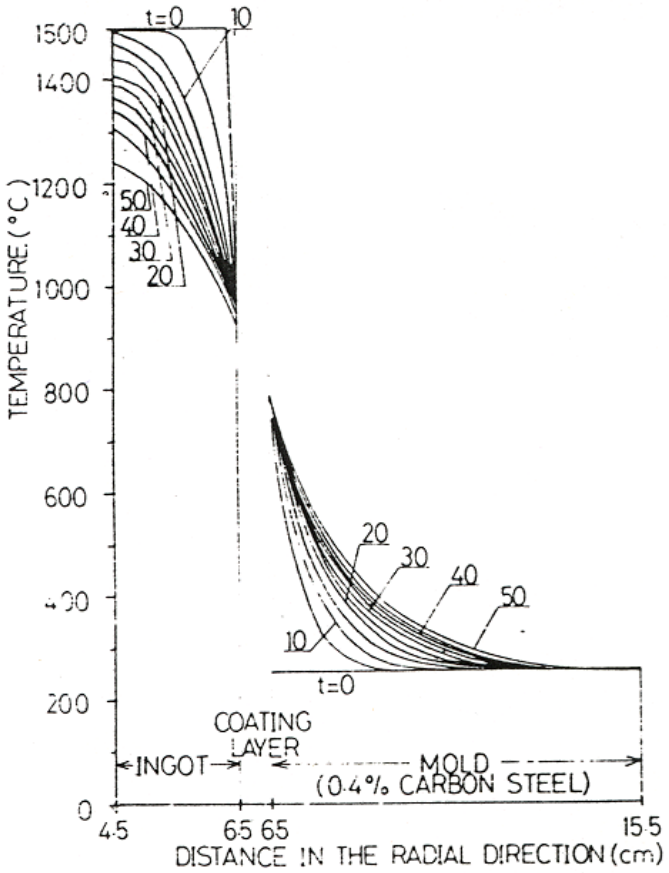

Fig 5.19. Temperature distribution in casting and mold region [Ebisu, 1977]

5.4 Results Obtained by ANSYS

The thermal analysis of developed model has been done in the Ansys to validate the results obtained by program, and results available in the literature. Due to geometrical symmetry of centrifugal casting, the two dimensional model has been developed for the given geometry in radial and longitudinal direction. The plane-77 thermal element has been chosen for the meshing of model. The appropriate boundary conditions and initial conditions are imposed on the model, and the transient thermal analysis of the model has been done. The node at the inner surface of the casting has chosen for the analysis, and the variation of temperature with time at that node, has been shown in the following graph. It is clear from the graph that temperature at that node falls below the solidus temperature (1300 ^{0}C) between time 50 seconds and 75 seconds. It is also evident from the figures that the whole casting solidifies in the time between 51seconds and 61 seconds. The figures show the temperature distribution in the

casting and mold regions for the different times. The trend of temperature profiles obtained by program and Ansys are similar and solidification time is also in the limit of foundry practice.

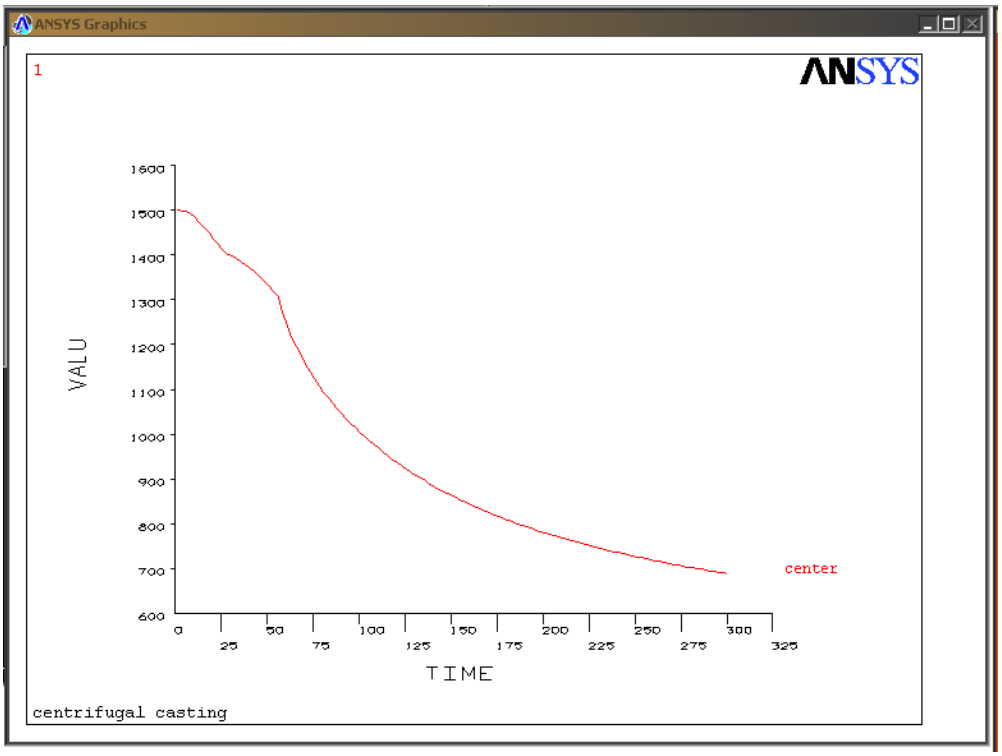

Fig5.20 Temperature variation at node, located at the inner surface of casting

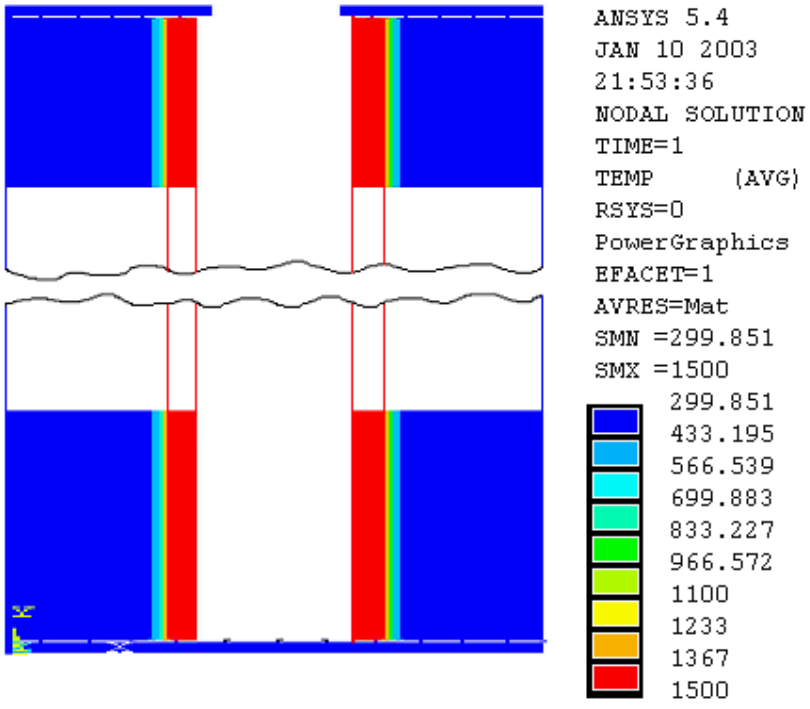

Fig5.21 Temperature distribution in the casting and mold region after time 1 sec

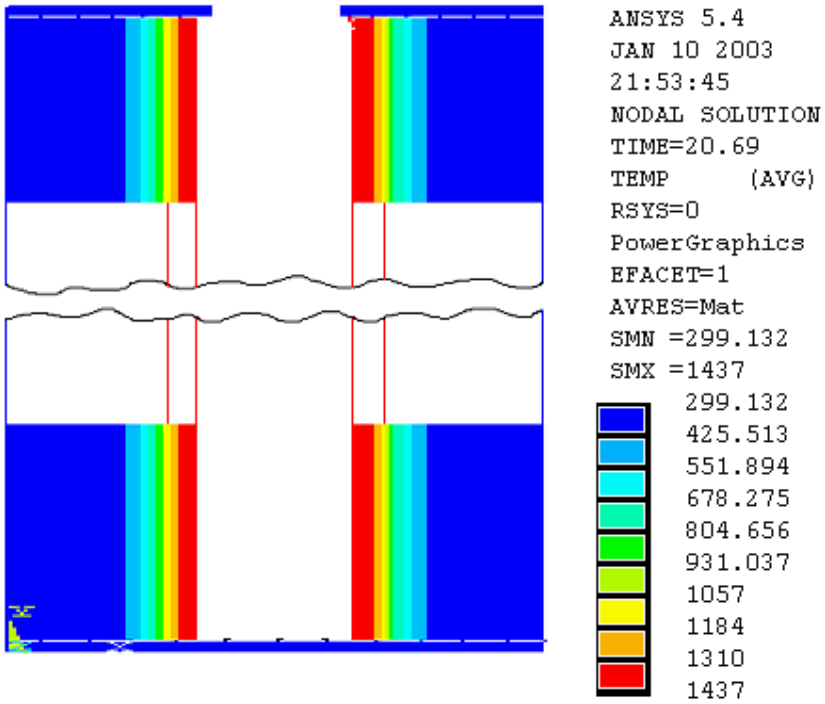

Fig5.22 Temperature distribution in the casting and mold region after time 20.69 sec

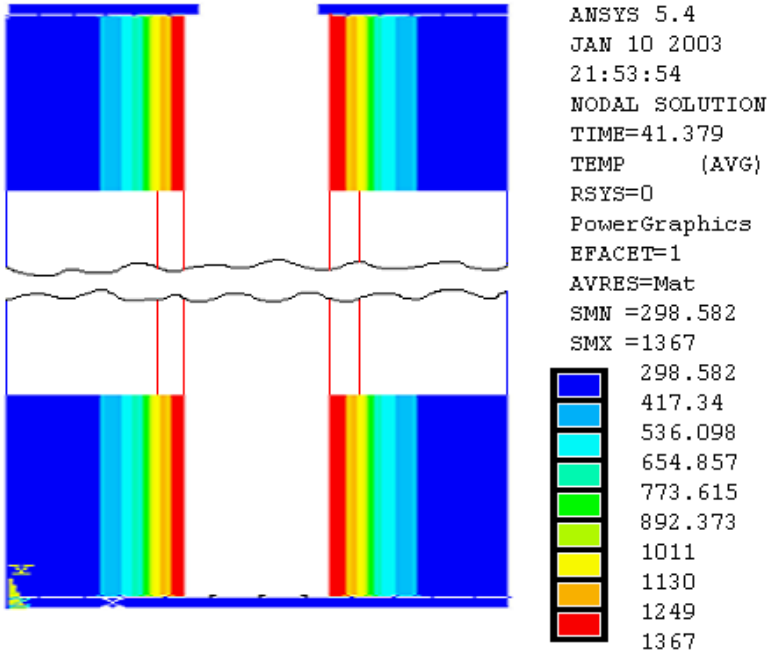

Fig5.23 Temperature distribution in the casting and mold region after time 41.379 sec

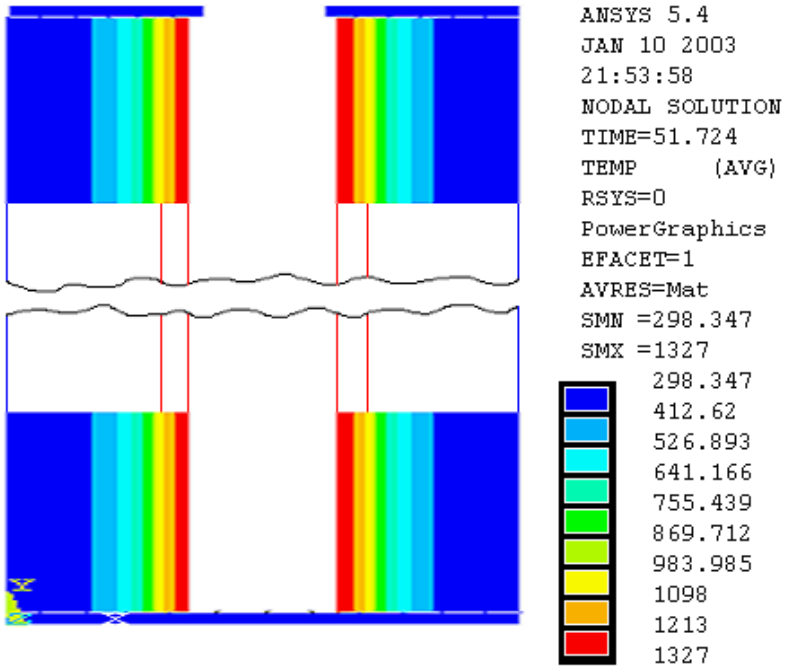

Fig 5.24 Temperature distribution in the casting and mold region after time 51.724 sec

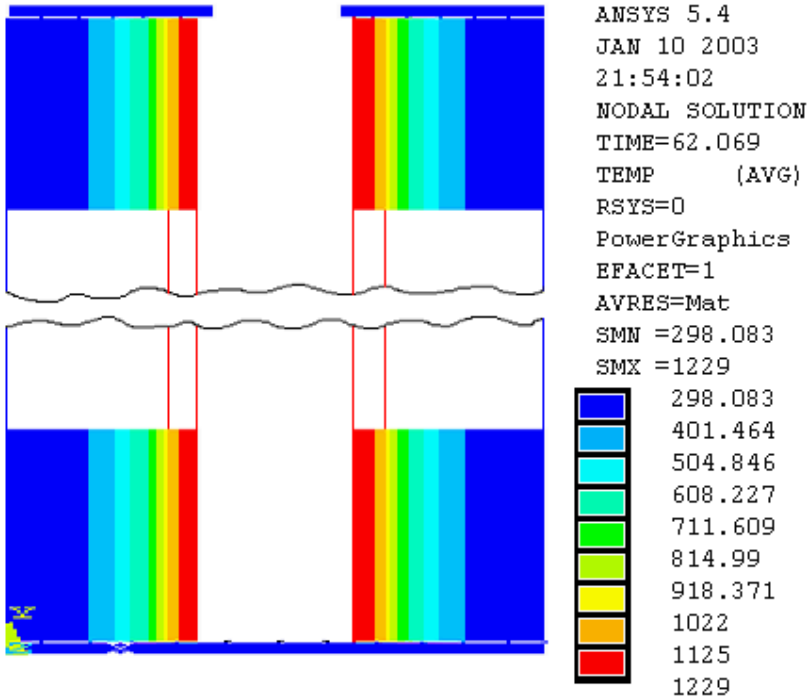

Fig 5.25 Temperature distribution in the casting and mold region after time 62.069 sec

Chapter-6

Conclusion

A mathematical model based on the heat transfer and solidification considerations has been formulated to simulate the centrifugal casting process. Model equations include energy balance for various zones. Firstly the model was solved using enthalpy formulation method to obtain the temperature profile in casting and mold region, and to find out the total solidification time. Then in order to find out the interface location in the radial direction model equation was solved by variable domain method. In this method to make the model more general and also to work in a domain of unchanging size in which the grid can be fixed once and for all, the heat transfer equations and boundary conditions for the casting region are written in terms of dimensionless variables.

For the solution of model equations explicit finite difference scheme with enthalpy method and implicit finite difference scheme with variable domain method is adopted. The resulting equations are arranged in a tridiagonal matrix form and are solved by using Thomas Algorithm. In the variable domain method, in order to find the solidification time for each segment, an iterative procedure, called modified variable time step (MVTS) approach has been used. The model equations have been solved in one dimension in radial coordinate system and for unit length of the cylinder.

Based on simulation results, following conclusions are drawn:

- The numerical program presented in this report provides a satisfactorily accurate method of simulating the solidification behavior of centrifugal castings. It is rational to consider that after air/gap formation heat is transferred by conduction whose ‘efficiency’ then decreases as solidification proceeds.
- A higher superheat of melt requires more time to solidify the metal. The pouring temperature has significant influence on solidification time along with other parameters.

- The initial temperature of the mold (preheating temperature) has a significant influence on the solidification time depending upon the relative value of interfacial heat transfer coefficient.
- The major factors affecting the solidification of centrifugal casting are pouring temperature of molten metal, mold preheat temperature, coating layer of insulation, rotational speed of mold, and heat transfer between the mold-metal interface during solidification.
- As the heat transfer at the metal-mold interface decreases due to formation of air gap, there is local heating effect in the outer region of the casting and local cooling effect at the inner surface of the mold.

Future Scope of Project

- The present model has been developed for only one dimension (radial direction), but since longitudinal temperature distribution also has significant effect on the mechanical properties of centrifugal casting, so for more realistic simulation above developed model should be solved in two dimensions.
- In the present model the heat transfer due to conduction in various regions is only considered, the consideration of convective heat transfer in liquid region can significantly increase the accuracy of results.
- Such a transient heat transfer model can also be exploited further to predict the time-temperature information which if correlated with the time-temperature-transformation diagram of a specific alloy system may lead to significant information about the microstructure of the developed casting.

References

1. Basu, B., and Date, A.W., "Numerical Modelling of Melting and Solidification Problems-A Review", *Sadhana*, *Indian Academy of Science*, Vol-13, Part-3, pp 169-213, 1988.

2. Bonacina, C., Comini, G., Fasano, A., and Primicerio, M., "Numerical Simulation of Phase Change Problems", *International Journal of Heat and Mass Transfer*, 16, pp1825-1832, 1973.

3. Choi, S.H., Kang, C.S. and Loper, C. R., "A study of the bonding of stainless steel to cast iron in centrifugal casting", *AFS Transactions*, pp 971-981, 1989.

4. Crank, J., and Crowley, A.B., "Isotherm Migration along Orthogonal Flow Lines in Two dimensions", *International Journal of Heat and Mass Transfer*, Vol-21, pp 393-398, 1978.

5. Crank, J., and Gupta, R.S., "Isotherm Migration Method in Two dimensions", *International Journal of Heat and Mass Transfer*, Vol-18, pp 1101-1107, 1975.

6. Crowley, A. B., "Numerical Solution to Stefan Problems", *International Journal of Heat and Mass Transfer*, 21(2), pp 215-219, 1978.

7. Cumberland, J., "Centrifugal Casting Techniques", *The British Foundryman*, pp 26-46, 1963

8. Ebisu, Y., "Computer simulation on Macrostructure in Centrifugal Castings", *AFS Transactions*, pp 643-655, 1977.

9. Gao, J. W. and Wang, C. Y., "Modeling the Solidification of Functionally Graded Materials by Centrifugal Casting", *Material Science and Engineering*, A292, pp 207-215, 2000.

10. Gupta, R.S., and Kumar, D., "Variable Time Step Methods for One Dimensional Stefan Problem with Mixed Boundary Condition", *International Journal of Heat and Mass Tansfer*, Vol-24, pp 251-259, 1981.

11. Hiene, R.W., and Rosenthal, P.C., "Principle of Metal Casting", *McGraw-Hill*, *New York*, 1955.

12. Howson, H.O., "Macrostructural Comparision of Centrifugal and Static Castings", *Foundry Trade Journal*, pp 261-272, 1969.

13. Janco, N., " Centrifugal Casting", *American Foundrymen's Society*, 1988.

14. Jones, M. C., "Investigation of Centrifugal Casting Techniques", *Foundry Trade Journal*, pp 1003-1017, June 18, 1970.

15. Kang, C.G.and Rohatgi, D.K.,"Transient Thermal Analysis of Solidification in Centrifugal Casting for Composite Materials containing Particle Segregation", *Metallurgical and Materials Transactions B*, vol. 27B, pp 277-285, April, 1966.

16. Kendoush, A.A., "An Approximate Solution of the Convective Heat Transfer from An Isothermal Rotating Cylinder", *Int. J. Heat and Fluid Flow 17*, pp 439-441, 1996.

17. Lazardis, A., "A Numerical Solution of the Multi-Dimensional Solidification (or Melting) Problem", *International Journal of Heat and Mass Transfer*, Vol-13, pp 1459-1477,1970.

18. Marrone, R.E., "Numerical Simulation of Solidification", *AFS Cast Metals Research Journal*, pp185-188, 1970.

19. Meyer, G.H., "Multi-dimensional Stefan Problems", *SIAM Journal of Numerical Analysis*, 10(3), pp 353-366, 1964.

20. Paranjpe, D.V., "Centrifugal Casting", *Foundry*, May/June, 2001.

21. Phelke, R.D., Kirt, M.J., Marrone, R.E., and Cook, D.J., "Numerical Simulation of Casting Solidification", *AFS, Illinois*, pp 1-7, 1974.

22. Raju, P. S. S. and Mehortra, S.P.,"Mathematical Modeling of Centrifugal Casting of Metal-Matrix Composites", *Materials Transactions, JIM*, vol.41, No.12, pp 1626-1635, 2000.

23. Saitoh, T. "Numerical Method for Multi-Dimensional Freezing Problems in Arbitrary Domains", *Tans. ASME, Journal of Heat Transfer*, Vol-100, pp 294-299, May 1978.

24. Shamsunder, N., and Sparrow, E. M., "Analysis of Multi-Dimensional Conduction Phase Change via Enthalpy Model", *Journal of Heat Transfer*, Vol-97, pp 333-340,1975.

25. Sparrow, E.M., Ramadhyani, S., and Pathankar, S.V., "Effect of Sub-Cooling on Cylindercal Melting", *ASME, Journal of Heat Transfer*, Vol-100, No.2, pp 395-402, 1978.

26. Szekeley, J., and Themlis, N.J., "Rate Phenomena in Process Metallurgy", *Wiley Interscience*, New York, 1970.

27. Upadhya, G., and Paul, A.J., "Solidification Modeling: A Phenomenological Review", *AFS Transactions*, pp 75-80, 1994.

28. Yang, B.J., Liu, W. T. and Su, J. U., "Numerical Simulation and Experimental Investigation of the solidification of Centrifugally Cast Cylinder Sleeves", *AFS Transactions*, pp 763-768, 1994.

Bibliography

i. Chapra, S.C. and Canale, R. P., "Numerical Methods for Engineers", *Tata McGraw-Hill*, 2000.

ii. Hoffmann, K.A., and Chiang, S.T., "Computational Fluid Dyanamics for Engineers", *Engineering Education Sys*., USA, Vol.1, 1995.

iii. Patankar, S.V., "Numerical Heat Transfer and Fluid Flow", *McGraw-Hill*, New York, 1980.

iv. Shamsunder, N., Wilson, D.G., Solomon A.D., and Boggs, P.T., "Comparision of Numerical Methods for Diffusion Problems with Moving Boundary", *Moving Boundary Problems*, Academic Press, New York, pp-165-183, 1978.